Cretaceous Eustasy Revisited

Article *in* Global and Planetary Change · January 2013

DOI: 10.1016/j.gloplacha.2013.12.007

CITATIONS
848

READS
9,553

1 author:

Bilal U Haq
Sorbonne University - Paris
141 PUBLICATIONS **21,613** CITATIONS

SEE PROFILE

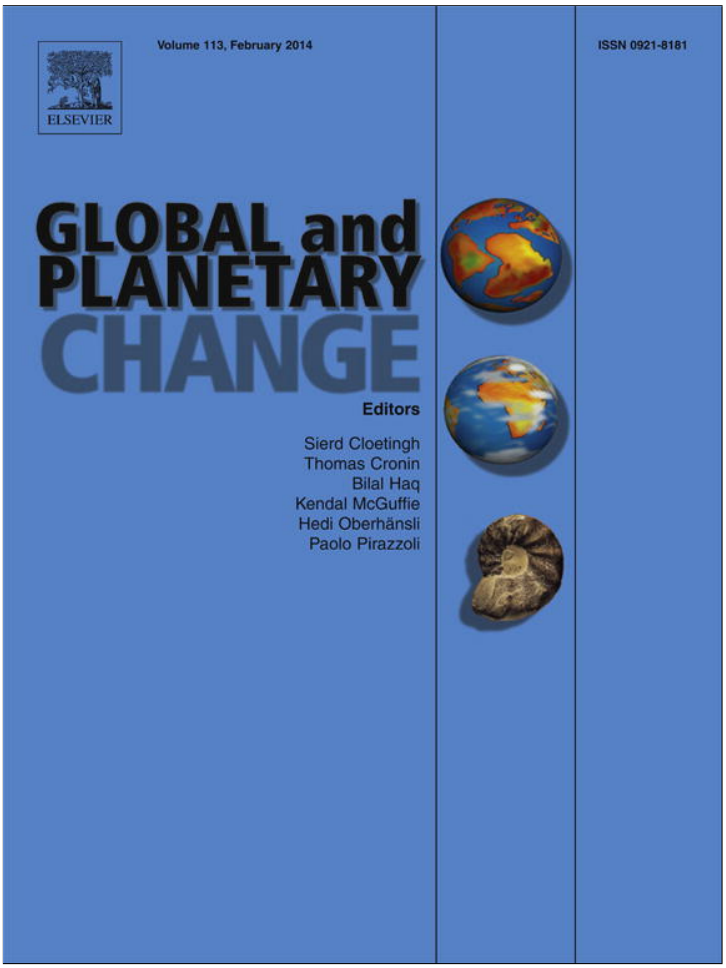

Global and Planetary Change 113 (2014) 44–58

Contents lists available at ScienceDirect

Global and Planetary Change

journal homepage: www.elsevier.com/locate/gloplacha

Review paper

Cretaceous eustasy revisited

Bilal U. Haq *

National Science Foundation, Washington, DC, USA, and Université Pierre et Marie Curie, Paris, France

ARTICLE INFO

Article history:
Received 9 December 2013
Accepted 17 December 2013
Available online 23 December 2013

Keywords:
Eustatic sea level
Cretaceous eustasy
Amplitude of sea-level changes

ABSTRACT

Eustatic sea-level changes of the Cretaceous are reevaluated based on a synthesis of global stratigraphic data. A new terminology for local/regional or relative sea-level changes (*eurybatic* shifts) is proposed to distinguish them from global (*eustatic*) sea-level changes, with the observation that all measures of sea-level change in any given location are eurybatic, even when they include a strong global signal. Solid-earth factors that influence inherited regional topography and thus modify physical measures of amplitude of the sea-level rises and falls locally are reviewed. One of these factors, dynamic topography (surface expression of mass flow in the upper mantle on land- and seascapes), is considered most pertinent in altering local measures of amplitude of sea-level events on third-order time scales (0.5–3.0 Myr). Insights gained from these models have led to the reconciliation of variance between amplitude estimates of eurybatic shifts in any given region and global measures of eustatic changes. Global estimates of third-order events can only be guesstimated at best by averaging the eurybatic data from widely distributed time-synchronous events. Revised curves for both long-term and short-term sea-level variations are presented for the Cretaceous Period. The curve representing the long-term envelope shows that average sea levels throughout the Cretaceous remained higher than the present day mean sea level (75–250 m above PDMSL). Sea level reached a trough in mid Valanginian (~75 m above PDMSL), followed by two high points, the first in early Barremian (~160–170 m above PDMSL) and the second, the highest peak of the Cretaceous, in earliest Turonian (~240–250 m above PDMSL). The curve also displays two ~20 Myr-long periods of relatively high and stable sea levels (Aptian through early Albian and Coniacian through Campanian). The short-term curve identifies 58 third-order eustatic events in the Cretaceous, most have been documented in several basins, while a smaller number are included provisionally as eustatic, awaiting confirmation. The amplitude of sea-level falls varies from a minimum of ~20 m to a maximum of just over 100 m and the duration varies between 0.5 and 3 Myr. The causes for these relatively rapid, and at times large amplitude, sea-level falls in the Cretaceous remain unresolved, although based mainly on oxygen-isotopic data, the presence of transient ice cover on Antarctica as the driver remains in vogue as an explanation. This idea has, however, suffered a recent setback following the discovery of pristine foraminiferal tests in the Turonian of Tanzania whose oxygen-isotopic values show little variation, implying absence of glacioeustasy at least in the Turonian. The prevalence of 4th-order (~400 Kyr) cyclicity through most of the Cretaceous (and elsewhere in the Paleozoic, Jurassic and Cenozoic) implies that the periodicity on this time scale, presumably driven by long-term orbital eccentricity, may be a fundamental feature of depositional sequences throughout the Phanerozoic.

Contents

* 4201 Wilson Blvd., Arlington, VA 22230, USA.
E-mail address: bilhaq@gmail.com.

0921-8181/$ – see front matter © 2014 Elsevier B.V. All rights reserved.
http://dx.doi.org/10.1016/j.gloplacha.2013.12.007

1. Introduction

Stratigraphy, like other natural sciences, endeavors to uncover concealed patterns in nature. In investigating eustasy we search for global patterns of sea-level change with time as they are preserved in the stratigraphic record. Ever since the notion of variable eustasy was first formally introduced by Eduard Suess is the late nineteenth century there have been both enthusiastic supporters as well as eager detractors of this concept. Nonetheless, the soundness of eustasy as a valid geological precept (at various time scales) has been widely demonstrated by extensive stratigraphic and paleoclimatological evidence, even though we still have not fully fathomed all the processes capable of producing a global signal at some time scales. In this paper a revised model of eustatic patterns for the Cretaceous Period (145–66 Ma) is presented (based on a synthesis of available stratigraphic data), together with an attempt to understand why sea-level events, even when they show consistency in timing, can exhibit variance in amplitude of rises and falls when measured physically at different locations.

The Cretaceous was first suggested as a geological subdivision in 1822 by d'Omalius-d'Halloy who dubbed the chalky sediments (*craie*) of Paris Basin *terrain crétacé*. It turned out that this was an appropriate designation for strata from an interval that is characterized by widespread occurrence of carbonate rocks deposited in the warm tropical/subtropical shallow seas, as well as mid to high latitude deep-sea environments. Study of Cretaceous paleoclimates and paleoceanography has seen renewed interest in recent years because of the high atmospheric CO_2 content and largely greenhouse climates of this Period, which are often cited as analogs of conditions projected for the near future of our planet resulting from current climatic trends. Stratigraphers have known for a long time that the Late Cretaceous was characterized by high sea levels worldwide, perhaps the highest in the Phanerozoic. What is less well recognized is the fact that coincident with these high eustatic levels the Late Cretaceous also saw the beginning of a shift in bulk of carbonate deposition from shallow to the deeper seas, a trend that continued into the Cenozoic (Southam and Hay, 1981), thereby changing the ocean's calcium carbonate saturation profile and enhancing the connection between interior seaways with the open ocean system (Ridgewell, 2005; Hay, 2008). These general characteristics make the Cretaceous of high interest to the hydrocarbon industry because of the presence of extensive petroleum systems within this period in the interior basins as well as offshore. Both reservoir and source rocks in stratigraphic traps of this age are currently coveted targets of exploration in many parts of the world. Useful recent reviews of the Cretaceous Period and discussions of its paleoclimate and paleoceanography have been provided by Gale (2000) and Hay (2008).

A knowledge of the chronology of past sea-level changes as recorded along continental margins and in the interior basins is considered indispensable by explorationists because it allows them to anticipate such exploration criteria as the frequency of base-level rise and fall and the duration of subaerial exposure (particularly important in carbonate environments that were common in the Cretaceous). A known schedule of past sea-level fall events can provide valuable clues about the extent of the migration of facies in response to base-level movements, as well as information about the degree of diagenesis in carbonates and thus their reservoir quality. The record of relative magnitude and duration of each highstand and knowledge of local morpho-dynamics can also allow valuable inferences about expected organic productivity and the preservation of source rock. This makes a cycle chart of past sea-level variations an essential component of an explorationist's tool box.

A previous Cretaceous cycle chart of sea level changes based on global stratigraphic data was published in the late 1980s as a part of Mesozoic–Cenozoic synthesis (Haq et al., 1987, 1988). The age model of that chart was updated by Hardenbol et al. (1998), who also compared the Cretaceous global sea-level fluctuations of Haq et al. (1987) to those from the European basins. Haq and Al-Qahtani (2005) further updated the chronology of events depicted on the cycle chart, tying them to the latest available time scale. Miller et al. (2004, 2008) documented the Late Cretaceous sea-level variations along New Jersey continental margin as a part of their study that focused on the last 100 Myr interval. They did not find the timing of the sea-level events (as gleaned from the New Jersey data) to be at variance with Haq et al. (1987), but estimated the amplitude for these events to be much smaller on New Jersey margin (even before applying "backstripping" corrections). This difference in amplitude estimates, i.e., those averaged from global data vs. those estimated from individual margins or basins, such as New Jersey or the Russian Platform (Sahagian et al., 1996), can now be more readily explained in view of the recent insight into morphodynamical changes that result from responses to long wave-length crustal warping related to *dynamic topography* along continental margins and in interior basins (discussed later in the paper).

1.1. Why revisit the Cretaceous?

A fresh look at the Cretaceous sea-level changes on a global basis is timely. The main rationale for this reconsideration is that since 1987 (the date of the last global synthesis for this interval) we have seen a considerable expansion of sequence-stratigraphic studies of Cretaceous profiles with well-defined biostratigraphies and documented sea-level fluctuations that can lend themselves to a global synthesis (especially data from those basins where the influence of short-term tectonics can be corrected for). The other reason for this revisit is the improvements in time scale for the Cretaceous. This time scale has been in a considerable state of flux, for example, compared to the Cretaceous time scale updated as recently as 2004 by Gradstein et al. (GTS, 2004) the latest revision published in 2012 (Ogg and Hinnov, in GTS 2012) revises almost all of the Cretaceous Stage boundary ages and their durations. In this revision the Early Cretaceous Valanginian Stage expanded by 1.7 Myr at the expense of Hauterivian, which shrank to less than half its earlier duration (3.1 Myr vs. 6.4 Myr in earlier version) and Barremian that also shrank by 0.5 Myr. In the Late Cretaceous the Cenomanian expanded by 0.5 Myr, Santonian by 0.4 Myr and Maastrichtian by 1.0 Myr at the expense of Campanian, which contracted by 1.4 Myr. In spite of these adjustments, there is near-consensus among stratigraphers that the Campanian Stage remains least well constrained (and perhaps still too long in duration), due to uncertainties that may exist because of the lack of well-preserved and complete sections for this interval. Also, so far only the last 8 Myr of the Cretaceous (latest Campanian and Maastrichtian) have been cyclostratigraphically tuned and as similar efforts continue for sections in deeper time, further refinements are very likely. GTS 2012 (Gradstein et al., 2012), nevertheless, is a vast improvement over the time scales available in 1987. Also, more reliable cross-correlations of biozones based on various fossil groups (and in different hemispheres and depositional realms) are now available, largely due to the herculean efforts of Hardenbol et al. (1998) assisted by an international team of specialists, as well as those summarized in Ogg and Hinnov (2012). This makes an attempt to synthesize events on a global scale considerably more effective and meaningful than was possible in 1987. In this paper we have recalibrated all of the global data to the Cretaceous time scale revision in GTS2012 (Ogg and Hinnov, 2012).

1.2. Introduction of new term: "eurybatic" shifts of sea level

The term *eurybatic* was first introduced by the author at the Cretaceous Symposium in September 2013, in Ankara, Turkey. This term is formalized here (in lieu of such terms as "relative", "local" or "regional" sea-level changes) with the realization that the measure of amplitude of sea-level changes (rises and falls measured in meters) are always local (i.e., *eurybatic*), even when there is a strong underlying global signal, since this measure at any given location is a product of both local vertical movements and eustasy (see discussion later in the paper). Thus, contrasting with *eustatic* (which implies sea-level variations of global extent), *eurybatic* is a term proposed for local or relative sea-level changes only (including the local/regional measure of the global, or *eustatic*, signal). The adjective *eurybatic* is derived from the name *Eurybia*, a goddess in Greek mythology, with power over sea level fluctuations. She was, appropriately, herself an offspring of Pontos (the sea god) and Gaia (the earth goddess) and includes divinities with power over elements such as winds, waves, and lunar and celestial influences among her descendants (all implicated in oceanic activities).

2. Factors affecting sea-level changes

In the literature on sea-level change there is a lot of confusion arising from inattention to time scales, even though it is widely recognized that the sea level varies at all timescales, i.e., from centennial to multi-million years. The factors that may be extremely relevant at shorter time scales (and of local import) affecting eurybatic measurements (e.g., isostatic response of landscapes and adjacent seascapes to glacial loading and unloading that operate at 10^2 to 10^3 years' time scales), may have much less pertinence on the longer time scales (e.g., 10^6 years or more). Yet, often these chronological distinctions are ignored in the discussion of sea-level variations. When discussing sea-level change, it is therefore important to specify the time scale of the events under consideration. Several interdependent methods of estimating the long-term sea level changes (on time scale of >10 Myr) are now available, e.g., those estimated from continental flooding data, or based on variations in the mean age of the seafloor (available as far back as the Cretaceous), models of mid-ocean ridge volume and length variations, emplacement of seamounts and large igneous bodies on the seafloor, and the potential use of oxygen-isotopic data as a proxy for ice volume (the latter is deemed as less suitable for deep time, see discussion later in the paper). However, here we are not only concerned with the long-term trends (also known as second-order variations) but also those over the relatively shorter term (spanning 0.5 to 3 Myr, or third-order changes) that are largely measured stratigraphically along continental margins and in the interior basins. We therefore need to be cognizant of all the stratigraphic and tectonic factors that influence these regions.

Broadly speaking, global sea level change can in two ways. 1) By changes in the amount of water in the ocean, which includes the glacial sequestration of water in ice caps and subsequent deglaciations, and the possibility of variations (or imbalance) of the ocean's water exchange with the deep mantle. Water exchange with mantle may be relevant over very long time scales (at planetary evolution times scales), but this exchange is generally assumed to be in balance for the Phanerozoic (i.e., water released from mantle into the ocean by degassing vs. water subducted down with hydrated minerals), though it may not be so during periods of anomalously high oceanic crustal production rates such as the Cretaceous (Conrad, 2013). During such intervals there may be a temporary net gain in the amount of ocean water, to be eventually balanced by subduction after a time lag. 2) Sea level can also change by changes in the volume of ocean basins (i.e., solid earth or tectonic influences on the seafloor or the continents, especially along their margins). Conrad (2013) has recently appraised us of the solid-earth factors that can affect sea-level changes in a thorough review, where he draws our attention to how newer tomographic images of deep earth and geodynamical modeling efforts of the last three decades have led to the realization that the global signal of sea level variations is expressed differently in different places due to regional lithospheric deflections that occur on all time scales. However, one potential missing factor in the review is the role of intraplate deformation and associated differential vertical motions that may also be important in determining resultant landscapes (Cloetingh et al., 1985). In addition, Cloetingh et al. (2013) have pointed out more recently that the wavelength and the magnitude of lithospheric warping due to intraplate deformation and lithosphere–mantle interactions depends strongly on the rheology of the lithosphere, which has been largely ignored in geodynamic models.

On the shorter time scales, the essentially geologically instantaneous elastic isostatic response to ice and water unloading (10^1–10^2 years), and what follows as the viscous post-deglaciation response (10^3–10^5 years) are both relevant for mass redistribution and thus regional vertical movements along the continental margins (Farrell and Clark, 1976; Conrad and Hager, 1997; Mitrovica et al., 2001). These therefore influence our measurement of the eurybatic amplitudes on those short time scales. At the time scales of third-order sea-level changes (i.e., 0.5 Myr or more) *dynamic topography* (Mitrovica et al., 1989; Gurnis, 1990, 1992) becomes more relevant than at shorter time scales. Dynamic topography is the longer wavelength and longer duration mantle convection flow patterns (material upwellings and downwellings) that affect changes in regional topographies, and thus

influence the stratigraphic measure of eurybatic changes in many locations.

Sea level rises are driven by net contractions (and falls by expansions) of the ocean container volume and these can be brought on by various manifestations of mantle convection on the longer time scales. The latter can express itself through changes in the volume of mid-ocean ridges (changes in the rates of spreading and thus the ridge size, as well as ridge length), emplacement of large volume of igneous material of the seafloor [e.g., three large igneous plateaus were emplaced on the Pacific seafloor contributing to the eustatic highs in the Cretaceous (Ito and Clift, 1998)], and net dynamic uplift (or subsidence) of ocean floor due to dynamic topography (Conrad, 2013). In addition to seascapes, landscapes can also inherit topographic changes through the long distance influences of dynamic topography and these can affect lateral variations in eurybatic measurements by warping the continental margins locally. A good example of this phenomenon is provided by its effect on the US East Coast since the Cretaceous (see discussion below). Although the surficial response to mantle convection forces has been envisioned since the late 1980s (e.g., Mitrovica et al., 1989; Gurnis, 1992), much of the detailed conceptual framework and modeling of this process and how it influences landscapes and seascapes post-dates the stratigraphic analyses of sea level along continental margins. One major advance made due to geodynamic modeling in the last two decades is the awareness of the role of dynamic topography, which has led to the recognition of reasons for the variance between estimates of eurybatic eustatic amplitudes.

2.1. Dynamic topography

An overview of dynamic topography (modeling as well as empirical data) has been recently provided by Flament et al. (2012). They define dynamic topography as the induced surface expression of mantle flow originating from the upper thermal boundary of mantle convection. A measure of dynamic topographic effect is what remains once you have removed the shorter-term effect of isostasy due to loading/unloading of sediments, ice, water and crust/lithosphere from the observed topography. Thus, the landscape response to dynamic topography baffles simplistic measures of eustasy based on stratal patterns along any given continental margin even when corrections for local factors have been applied. Nevertheless, because the effects of dynamic topography on surface features become notably apparent only on the relatively longer time scales (>5 Myr), it can only dampen or enhance the underlying global signal of the third-order sea-level events that occur at shorter time scales and it rarely wipes out this signal completely. This is apparently what happened along the US East Coast, which provides an appropriate example of the influence of this factor because of the numerous modeling studies that followed the backstripped stratigraphic estimates along this margin.

Extensive and thorough stratigraphic and basin-analysis studies of New Jersey margin by K. Miller, M. Kominz and their colleagues (which included drilling both on land and offshore) have documented the sea-level history of this margin (e.g., Kominz et al., 1998; Miller et al., 1998, 2004, 2003, 2005a,b). Their backstripping treatment included corrections for water depth and subsidence induced by thermo-flexural warping as well as sediment loading and compaction. As mentioned earlier, their amplitude estimates for sea-level falls for third-order events resulting from these studies were considerably lower than the global-mean estimates of Haq et al. (1987). Miller and colleagues argued that the New Jersey margin has remained relatively stable since the Late Cretaceous and has not been influenced by disruptive tectonics, thus implying that sea-level variations as measured (and corrected) along New Jersey represent a better *eustatic* signal than the global-mean higher estimates. However, since then the cognizance of dynamic topographic factors has changed our views about the long-term stability of both the continents and their margins leading to the conclusion that *all physical measures of sea-level change in any given location are eurybatic!*

In a reconstruction of the bathymetry and age-area distributions of the ocean basins for the last 140 Myr Müller et al. (2008) arrived at estimates that were 45–230 m higher than those from New Jersey. They employed a mantle convection model that suggests that the New Jersey margin may have subsided between 105 and 180 m just in the last 70 Myr due to North America's passage over the subducted and negatively buoyant Farallon Plate that had been tomographically imaged in the lower mantle (e.g., Ritsema et al., 2004; Sigloch et al., 2008). The migration of the remnants of the Farallon Plate beneath North America has also been modeled by Liu et al. (2008), who have shown detailed versions of this dynamic passage and its surface effects since the Late Cretaceous. Thus, lacking the dynamic topographic corrections, Miller et al. (2004) could understandably have been led to underestimate the amplitudes of sea level falls along the New Jersey margin. And to their credit they did attempt to revise their estimates upwards after considering the potential effects of dynamic topography on the East Coast (Kominz et al., 2008), though their new numbers are still lower than the globally averaged estimates. Müller et al. (2008) further suggested that when corrected for this dynamically-induced subsidence, the Miller et al. (2005b) sea-level high at 80 Ma would change from ~75 m to 142–217 m above present-day sea level, approaching the global estimate of Haq et al. (1987). These conclusions about dynamic topographic effects on the subsidence of New Jersey margin have also been reinforced by other independent modeling efforts (e.g., Moucha et al., 2008; Spasojevic et al., 2008; Spasojevic and Gurnis, 2012; Rowley et al., 2013).

It has long been known (e.g., Mitrovica et al., 1989; Gurnis, 1992, 1993; Lithgow-Bertelloni and Gurnis, 1997) that most locations are subject to long-term dynamic vertical topographic motions. Spasojevic et al. (2008) reemphasized the role of dynamic subsidence of the US East Coast as a result of mantle convection. The latter also ascribed the discrepancy between amplitude estimates of the New Jersey sea-level events for last 100 Myr and the global estimates to dynamic subsidence. In a worldwide consideration of various factors that contribute to long-term sea level change, Spasojevic and Gurnis (2012) again indicated that their independently derived amplitude estimates are closer to the global stratigraphic estimates rather than those from New Jersey. Although the dynamic modeling study of Moucha et al. (2008) is limited to the last 30 Myr, its basic message is the same as the conclusions base on other modeling studies, i.e., the New Jersey margin illustrates the effects of the continued descent of the Farallon Plate and when corrected for dynamic subsidence produces sea-level variations that are comparable to the higher global estimates and are also within the constraints of the backstripping methodology. Mantle convection modeling of the US East Coast from Florida to Virginia for the last 3 Myr by Rowley et al. (2013) similarly came to the conclusion that dynamic topography makes it obvious that any local measure of sea-level change is regional and not global. These authors also emphasize the uncertainties inherent in various dynamic modeling parameters, which do not permit accurate estimation of the correction factors to apply for dynamic topography. As a result it is challenging to take a local measurement and extract a global long-term sea-level signal from it, or in turn estimate the size of the Antarctic ice sheet using US East Coast data (Rowley et al., 2013).

The above example is illustrative of the difficulty of teasing out a measure of the eustatic signal from eurybatic measurements in any given location. Thus, a better sense of third-order global variations has to come from consideration of widespread data, especially from distant non-contiguous basins, a measure of the global mean provided by averaging the amplitude of changes from time-equivalent events in all considered sections. Nevertheless, we still have to contend with the unhappy reality that this *sense* will always be an approximation, rather than approaching an accurate quantity. Use of foraminiferal oxygen isotopes initially held great promise in helping us with better amplitude

estimates, but that methodology also suffers from several problems, which confound ice-volume appraisals.

3. Foraminiferal oxygen isotopes as a proxy for ice volume

Oxygen isotope ($\delta^{18}O$) records from foraminifers are largely comprised of two dominant signals, i.e., ambient temperature and $\delta^{18}O$ of seawater. The latter parameter is affected by continental ice-volume and variations in regional evaporation and precipitation (i.e., salinity). Foraminiferal $\delta^{18}O$ measurements have been effectively used as an ice-volume (i.e., sea-level) proxy for the sub-Recent time scales ever since Emiliani (1955) proposed that foraminiferal oxygen isotopic values could be used to reconstruct ocean temperatures and Shackleton (1967) revised the magnitude of ice volume:$\delta^{18}O$ component proposed by Emiliani. If one can assume that Pleistocene sea level:$\delta^{18}O$ slope was similar across all geological time scales, then it might be possible to estimate the amplitude of past eustatic variations using this proxy. However, application of oxygen-isotopic paleothermometry to older (pre-Pleistocene) times for determining the amount of ice sequestered on continents is fraught with difficulties. This is not only because of the problems of not knowing the past oxygen-isotopic composition of seawater (normally accomplished by removing the temperature and local hydrological effects by determining Mg/Ca ratios of the same samples, which can then lead to estimates of $\delta^{18}O$ of sea water, see e.g., Lea et al., 2002), but also because of another inconvenient detail: developing ice sheets become progressively depleted in ^{18}O as elevation increases and temperatures decrease, thereby increasing $\delta^{18}O_{sw}$ by varying amounts. Thus, in early stages of growth, the mean $\delta^{18}O$ of the ice sheets are higher than at later stages. Also, when ice sheets wane, without melting completely, and wax again their mean isotopic values become even more difficult to decipher. In addition, there are other complicating factors, such as the pH variations (carbonate ion effect) on $\delta^{18}O$ of carbonate shells (Zeebe, 2001; Tyrrell and Zeebe, 2004), and diagenetic changes that can alter the $\delta^{18}O$ signal in some deep-time carbonates. These issues further complicate the use of oxygen-isotopic data effectively for quantitative measures of the amplitude of sea-level changes in the deep geologic past. At best these data can only provide us with a sense of relative magnitude of eustatic variations. Pearson (2012) has provided a very useful review of the history and nuances of use of oxygen isotopes in paleoceanography.

Nonetheless, because the benthic oxygen-isotopic signal clearly incorporates an ice-volume component, smoothed $\delta^{18}O$ curves have effectively aided in determining the *timing* of eustatic events (sea-level falls) in the past. A number of oxygen-isotopic curves for parts of the Cretaceous have been published over the past two decades (e.g., late Campanian–Maastrichtian, Li and Keller, 1998; Barrera and Savin, 1999; Li et al., 1999; late Albian–Maastrichtian, Huber et al., 1995, 2002; Barremian–early Aptian, Stoll and Schrag, 1996; Cenomanian–Maastrichtian, Abreu et al., 1998; late Albian–Santonian, Stoll and Schrag, 2000; middle to Late Cretaceous, Friedrich et al., 2012, among others). Of particular interest for the current discussion is the Late Cretaceous high-resolution oxygen-isotopic record from the Italian Contessa Section of Stoll and Schrag (2000). Although these data were obtained from bulk carbonate samples where diagenetic effects cannot be ruled out, the resulting curve shows a remarkable correlation to the third-order sea-level falls of Haq et al. (1987) with positive $\delta^{18}O$ excursions of 0.5 to 1.0‰. This led Stoll and Schrag (2000) to suggest that their data implies a robust ice-volume component and thus the Late Cretaceous coolings must have been accompanied by ice accumulations on Antarctica. Recently $\delta^{18}O$ data from Tanzania with extremely well-preserved foraminiferal tests (both planktonic and benthic species) that display no outward sign of diagenetic alteration show that the Turonian was relatively uneventful and stable with no evidence of a prominent positive $\delta^{18}O$ excursion, which the authors interpret to mean no glaciation on Antarctica at that time (MacLeod et al., 2013, B. Huber, personal communication, 2013). However, for the same interval the Contessa section (Stoll and Schrag, 2000) as well as sections elsewhere in the Tethys and North Atlantic region studied by other workers (e.g. Miller et al., 2004; Bornemann et al., 2008; Galeotti et al., 2009) showed a strong positive ~1.0‰ excursion, which correlates with a sea-level fall on the eustatic curve. Similarly, Ando et al. (2009) disputed the possibility of a glacial episode in the mid Cenomanian, as they saw no evidence of a $\delta^{18}O$ shift in data from the Blake Nose in western North Atlantic in that interval.

This then begs the question, what is causing this apparent similarity between third-order sea level and $\delta^{18}O$ curves? If it is not ice volume, then it must be an alternative co-varying process related to eustasy that modifies the $\delta^{18}O$ signal as sea level fluctuates. One could argue that compared to the pristine preservation in Tanzania, sections elsewhere have suffered diagenesis to a lesser or greater degree, especially the bulk samples from Contessa section analyzed by Stoll and Schrag (2000). Is it possible that the degree of diagenetic alteration (and the $\delta^{18}O$ signal) in bulk carbonates was controlled by sea level rises and falls? If this were true, then (in the absence of glaciation) it would make the diagenetically altered record more useful as a historical record of the sea-level fluctuations than a pristine record. The implications of this observation are significant and the similarity between $\delta^{18}O$ signal and third-order sea-level changes deserves more attention from geochemists and paleoceanographers to resolve this issue. [Another intriguing possibility for the differences between Tanzanian and Contessa records was offered by Howard Spero during a review of this aricle (personal communication. 2013), i.e., that this may be a reflection of the changes in evaporation/precipitation patterns that can produce relatively large $\delta^{18}O$ swings, as demonstrated by the study of meridional shifts in marine intertropical convergence zone and tropical hydrologic cycle over the last three glacial cycles by Schmidt and Spero (2011), and further documented recently by Arbuszewski et al. (2013) in the Atlantic].

In addition to the late Cretaceous data published by Stoll and Schrag (2000), bulk carbonate stable-isotopic data from the entire Contessa Section that covers nearly all of the Cretaceous Period (with the exception of the early Barremian) was generated by Dan Schrag and his colleagues (D. Schrag, personal communication, 2006) and was provided to the author. These data, which are tied to a well-constrained biostratigraphic framework, were rescaled to the most recent Cretaceous time scale (Ogg and Hinnov, 2012) and smoothed for a comparison with sea-level variations (see Fig. 3, in Appendix A). This comparison showed a close similarity between the timing of positive $\delta^{18}O$ excursions and globally identified sea-level falls of Haq et al. (1987) for all Late Cretaceous stages except the Campanian (where the number of events was comparable, but not the timing). The correlations for the Early Cretaceous events are also analogous and meaningful. This comparison indicates that conspicuous positive shifts of $\delta^{18}O$ may be able to aid us in narrowing down the timing of third-order eustatic falls, when such assignments are otherwise based on biozones with relatively longer durations (see Appendix A and Fig. 3, and further discussion of individual third-order events and the use isotopic data in narrowing their timing).

4. Construction of the long-term sea-level curve for the Cretaceous

As mentioned earlier, the long-term curves shown in Figs. 1 and 2 are mostly based on geophysical criteria while the shorter-term (third-order) events are essentially stratigraphically identified. Following the calibration established in previous published curves (Haq et al., 1987, 1988) in this paper the highest sea level of the Cretaceous at 93.5 Ma (earliest Turonian) has been scaled at ~240–250 m above present day mean sea level (or 180–190 m without the extant ice cap, which is estimated to hold water equivalent to another 60 m of sea-level rise). Scaling the long-term sea levels in the Cretaceous to this height (and to be higher than the Jurassic and Cenozoic) was considered meaningful

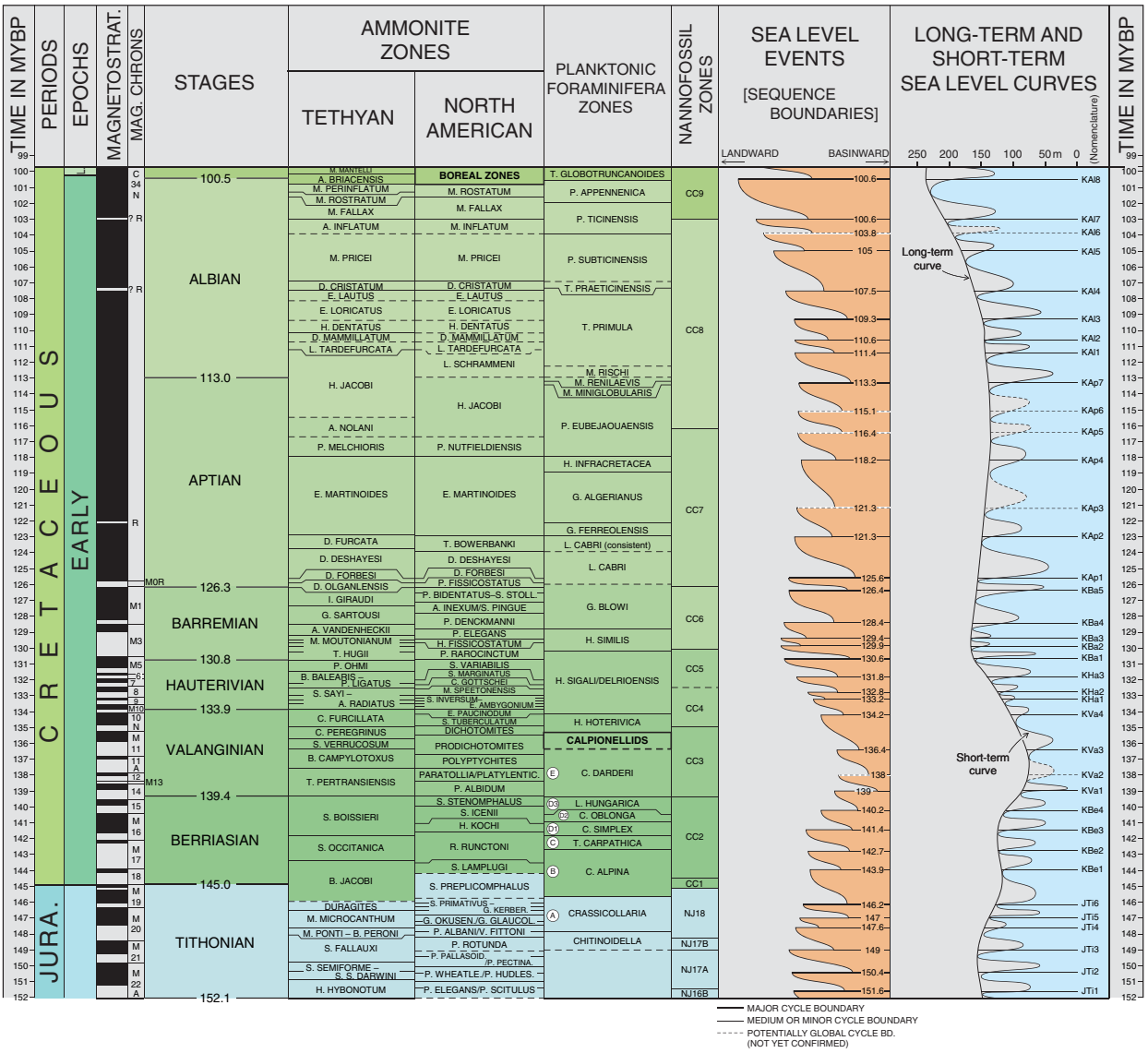

Fig. 1. Early Cretaceous Eustatic Cycle Chart tied to GTS2012. Cross-correlation of biozones are after Hardenbol et al. (1998) and Ogg and Hinnov (2012). The left half of the figure shows standard stratigraphic subdivisions calibrated to the absolute time scale and paleomagnetic reversal scale. The right half of the figure shows an onlap curve on the left, which is a measure of relative landward or basinward movement of the regional baseline as estimated from several sections. Estimated biochronological ages of the sequence boundaries are indicated for each event. On the right the sea level curves are shown, which include both the long-term envelope and the short-term (third-order) curve of sea level fluctuations. In the Nomenclature column Cretaceous sea-level fall events are numbered following the scheme suggested by Hardenbol et al. (1998) and also recommended by Snedden and Liu (2011). However, the letter **K** (for Cretaceous) has been prefixed to each number (**KBe1** to **KAl8**, see also Appendix A for explanation).

by Haq et al. (1987) largely in view of continental flooding data and high oceanic crustal production rates. Although our understanding of the vertical dynamics of continental margins and interior basins has since improved dramatically the effective estimate of the Cretaceous high remains unaffected. It must be underscored, however, that this measure is only a guesstimate at best and likely to remain so in view of the errors inherent in all methodologies discussed below. The current longer term curve is scaled after consideration of the following interrelated factors: 1) variations in the mean age of the oceanic lithosphere, 2) variations in the production rates at mid-ocean ridges, 3) episodes and duration of emplacement of seamounts and LIPS on the seafloor, 4) evolving sediment input into the ocean, 5) modeled global dynamic topographic considerations, and 5) continental flooding data (corrected for dynamic topographic effects).

The geodynamic modeling efforts of the last decade are relevant to the discussion of long-term sea-level trends. Cogné et al. (2006) modeled the mean age of oceanic lithosphere and compared it to the long-term eustatic curve. They surmised that when the effects of emplacement of the LIPS and glaciation are added to their model results, they fit the eustatic data well. They concluded that mean-age of the oceanic crust provides the primary (70%) control of the long-term sea level. Müller et al. (2008) made a more comprehensive reconstruction of global seafloor age-area and depth-area distribution for the last 140 Myr by also taking into account the subducted seafloor. They maintain that earlier attempts to reconstruct the past age-area distribution by assuming an average age/area similar to the present day and without including the subducted seafloor in the equation would have led to errors. In addition to the seafloor area and depth, they also considered the effects of changes in the crustal production, sediment input, as well as LIPS emplacements at 120, 110 and 90 Ma in the Cretaceous and came up with an estimated range of a late Cretaceous sea-level high of between 85 and 270 m (their best estimate ~170 m). Spasojevic and Gurnis' (2012) dynamic earth model simulations took into account seafloor

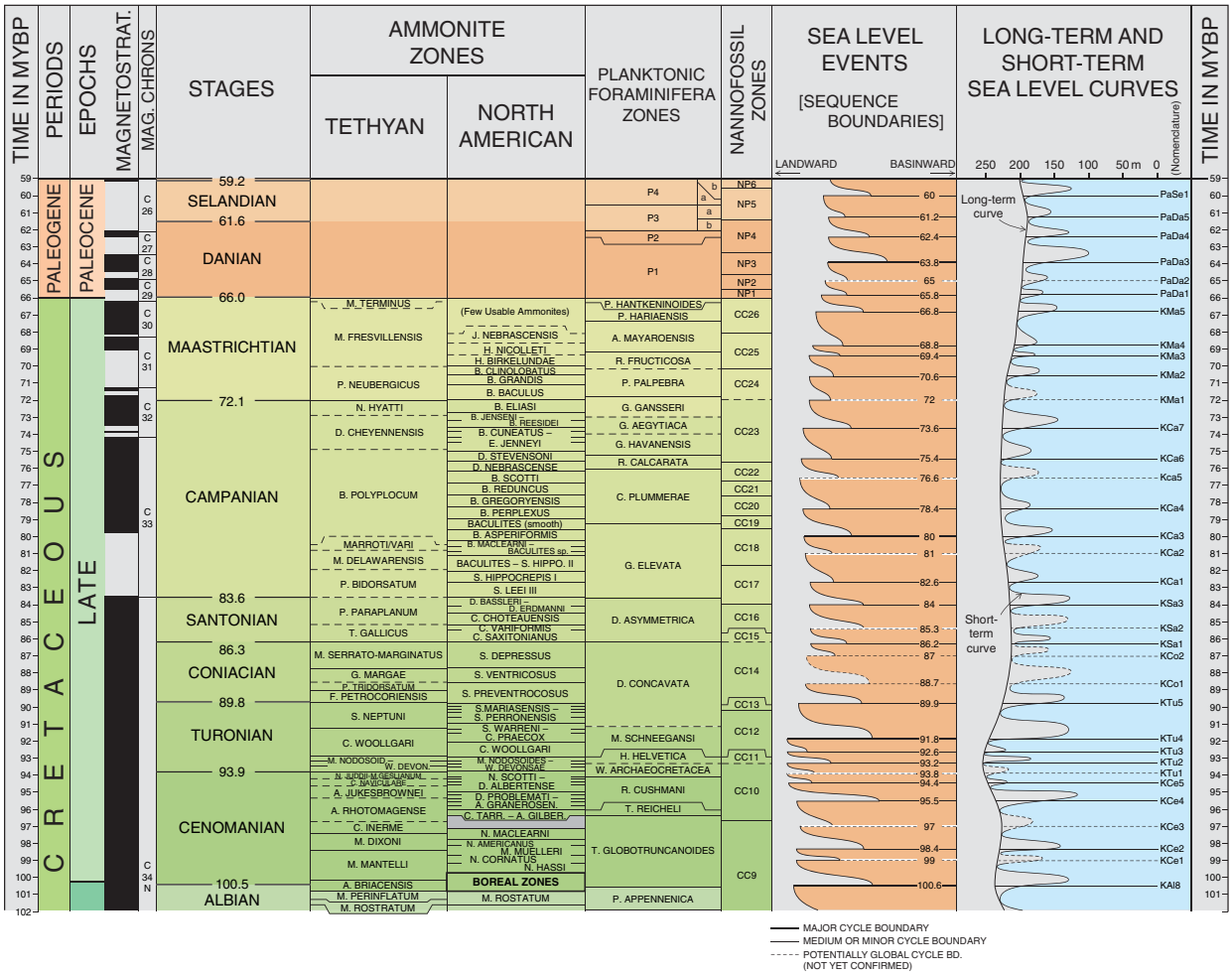

Fig. 2. Late Cretaceous Eustatic Cycle Chart. Cross-correlation of biozones are after Hardenbol et al. (1998) and Ogg and Hinnov (2012). Cretaceous events are numbered following the scheme suggested by Hardenbol et al. (1998) and also recommended by Snedden and Liu (2011), however, the letter K (for Cretaceous) has been prefixed to each number (**KCe1** to **KMa5**, see also Appendix A for explanation). See caption of Fig. 1 for a complete explanation.

age, crustal production rates, dynamic topography as well as geoidal variations and yielded a long-term overall eustatic fall of ~286 m since Late Cretaceous high. The most recent review of various solid-earth factors that influence sea level change by Conrad (2013), including ocean basin-area evolution, ridge-volume changes, seafloor volcanism, global dynamic topographic effects and sediment thickness came up with a net sea-level decline of ~250 m since the mid Cretaceous. It is apparent then that various empirical global estimates as well as modeling studies are now approaching a near-consensus that the eustatic highs in Cretaceous were in the range of 170–280 m above present day sea levels, this range being large in view of the inherent uncertainties of each methodology (discussed by Spasojevic and Gurnis, 2012 and Conrad, 2013).

5. Construction of the 3rd-order sea level curve for the Cretaceous

Documentation for the third-order events recorded on the shorter-term sea level curve is based mostly on sequence-stratigraphic data from around the world, and where possible, reinforced by oxygen-isotopic trends. As discussed earlier, we cannot rely on carbonate oxygen-isotopic values for quantitative amplitude measurement in the deep past. Nevertheless, these values can aid us in qualitative relative magnitude approximations, as well as in narrowing the timing of the sea-level fall events (i.e., sequence boundaries) (see Fig. 4).

In addition to the well-established criteria for sequence stratigraphic interpretations (see e.g., Sarg, 1988; Van Wagoner et al., 1988; Handford and Loucks, 1993), following lithological and paleontological criteria (originally listed by Haq and Schutter, 2008) have also aided in our interpretation of system tracts and depositional surfaces as well as sequence boundaries in outcrop sections:

5.1. Condensed section deposits

Transgressive facies occurring in the condensed section represent sediment starvation on the shelves while the depocenters move landward during transgression. These facies are usually rich in organic material and may also include authigenic minerals such as glauconite and phosphorite, and oolitic ironstones as well as marine shell and bone beds. Concentration of fossil material due to sediment starvation often makes the transgressive facies ideal for dating the sequence.

5.2. Transgressive coals

These occur as continuous sheet coals over a large area rather than being confined to a valley or a lake. They usually overlie rooted exposure

surfaces (sequence boundaries) and are in turn overlain by marine deposits.

5.3. Evaporites

Evaporites are often associated with carbonate systems. Relatively thick evaporites can be deposited both during the lowstands (when they are generally confined to the basin) and during the late highstands (on shelves and interior seaways). Caution should be exercised in their interpretation and vertical and horizontal relationships need to be examined to ascertain their occurrence as lowstand or highstand features.

5.4. Carbonate megabreccias

These lowstand features occur on slopes and along basin margins in carbonate systems. Caution should be exercised in their interpretation, since they can also be produced by an advancing thrust sheet or regressive progradation of the platform. When abruptly emplaced on or at the foot of the slope with no relationship to progradation, they can be interpreted as lowstand equivalents.

5.5. Exposure-related deposits

Surfaces with evidence of erosion and exposure are usually quite obvious but they can also be subtle when soil formation processes are less active. Incised valley fill deposits, autochthonous coals, eolian sandstones and karst in carbonates are some of the features related to exposure in the Cretaceous. In addition, laterite/bauxite deposits are indicative of extreme weathering of host rock during exposure in humid and warm climates.

5.6. Forced regressive facies

The phenomenon of forced regression (eurybatic shifts without normal progradation) can be relatively common when shorelines migrate rapidly and over long distances as a consequence of low topographic relief in cratonic interiors or on broad shelves. A forced regression of the shoreline is induced by stepwise base-level lowerings, setting off cannibalization of the coastal/near-shore sediments to form new coastal offlapping deposits.

5.7. Other helpful paleontological features

Changes in evolutionary and biogeographic patterns such as radiations and extinctions and faunal migrations in response to changing sea level are well established. For example, extinctions of shallow-marine faunas are more likely to occur during lowstands while landward migration of offshore biofacies is preceded by a sea-level rise. High sedimentation rate environments without subaerial exposure (as during a late lowstand) will sometimes conserve soft body parts of animals that would otherwise not be preserved in low sediment influx areas.

Estimating the relative magnitude of eurybatic shifts from sequence-stratigraphic data is also well established and not repeated here. In practice, however, it is rarely possible to acquire a precise measure of the amplitude of the eurybatic falls or rises. While it is often possible to determine the timing of baseline withdrawal beyond the extant shelf edge, it is challenging to measure the amount of eurybatic fall from stratigraphic data because of the unknown amount of erosion on the shelf associated with the withdrawal. A rise is even more difficult to quantify because of the possibility of incomplete filling of the depositional accommodation space during the highstand or because of partial or complete erosion of the highstand systems tract following the fall (Haq and Schutter, 2008). This implies that all amplitude assessments from physical data must be considered relative rather than absolute. As mentioned earlier, the backstripping method can help refine such estimates through corrections for sediment loading, and compaction and basin-floor subsidence (see e.g., van Sickel et al., 2004; Kominz et al., 2008). Nevertheless, these estimates are almost always bracketed by large error bars mostly due to considerable uncertainties introduced by factors mentioned above and long ranges of habitat depth of paleobathymetric-indicator benthic species as well as the potential for differential subsidence. In view of these issues, for amplitude assignments to the third-order events, an approach similar to that used by Haq and Schutter (2008) for the Paleozoic synthesis is adopted here. They derived the amplitude estimates for eustatic rises and falls by averaging eurybatic measurements from all the stratigraphic sections under consideration (based on stratigraphic measures such as thickness of system tracts, bio- and lithofacies depth assessments, the depth of incision on shelves and partial backstripping). In this synthesis, after ascertaining that timing of documented sea-level fall events is duplicated in at least three or more, preferably non-contiguous basins, the eurybatic amplitude estimates are averaged to obtain a sense of eustatic measure for each event. Since these measures are never precise, Haq and Schutter (2008) classified each event quasi-quantitatively (measured as the amount of fall from the previous highstand) as minor (<25 m), medium (25 to 75 m), or major (>75 m). This scheme is adopted here for the Cretaceous as well. From the worldwide data considered in the current synthesis it is evident that although the overall cumulative long-term eustatic high was as much as 240–250 m, the individual third-order falls rarely exceeded 100 m. All stratigraphic sections considered here (outcrops, well-logs as well as seismic profiles) have been recalibrated to the latest available Cretaceous time scale (Ogg and Hinnov, 2012) and the biochronological schemes for various fossil groups therein. After recalibration, the extensive cross-correlation results for biozonal schemes for both Tethyan and Boreal regions presented by Hardenbol et al. (1998) also proved exceedingly useful in the current synthesis.

6. Results and discussion

Results of the Cretaceous eustatic synthesis are presented in Fig. 1 (for the Early Cretaceous) and Fig. 2 (for the Late Cretaceous). The figures show the current (GTS 2012) radiometric time scale from Tithonian (youngest Jurassic Stage) through Danian (oldest Paleogene Stage) tied to paleomagnetic reversal scale, the standard Cretaceous Stage subdivisions and biostratigraphic zonal schemes commonly used in the temporal subdivision of Cretaceous. Ammonites are the most commonly utilized fossil group in the Cretaceous and thus both Tethyan (a region that encompasses western European basins through the Indian subcontinent) and North American zonal schemes are included based on cross-correlations provided by Hardenbol et al. (1998) and Ogg and Hinnov (2012). Planktonic foraminifers are the second most commonly used group, although many of these biozones tend to be of long duration. In the earliest Cretaceous (Berriasian through Valanginian) foraminifers are not very effective and instead Calpionellids are often substituted for the late Tithonian through Valanginian interval.

The chronostratigraphic scheme described above is plotted against the results of the current eustatic synthesis. The sea-level fluctuations are shown in two columns: the first column (to the left) shows these fluctuations as “events” which are essentially third-order sequence boundaries or sea level falls. Since the synthesis is based on sequence stratigraphic interpretations (or reinterpretations), the time-synchronous sequence boundaries in several non-contiguous basins are considered eustatic. The second column (to the right) shows the sea-level variations as the long-term and short-term (third-order) eustatic curves. The criteria for the long- and short-term curves have been discussed earlier. The amplitudes of third-order sea-level variations as shown here are averaged from stratigraphic estimates in several basins and as such should be considered approximate. The sections used for each event are listed in the Appendix A. Some events

included in the two columns are shown with dashed lines: these are included here provisionally as they do not fit the inclusion criteria strictly, but are suggested to be eustatic due to various reasons, which are discussed individually for each event in the Appendix A. These provisional events will have to await confirmation or rejection based on further stratigraphic studies in other areas.

One noticeable feature of the long-term envelope is that mean sea levels throughout the Cretaceous remains higher than the current sea level, i.e., between ~65 and ~250 m higher than the present day mean sea level (PDMSL). It should be noted that these estimates would change to ~5 to 190 m higher than PDMSL if they were calculated assuming an ice-free world (i.e., if all present day ice caps and glaciers were to melt, current global mean sea level would be ~60 m higher). The long-term curve also displays some very distinct variations. Mean global sea level starts off as relatively high (~150–160 m above PDMSL) in the latest Jurassic (Tithonian) but dips near the Tithonian–Berriasian boundary by 40–50 m. A further dramatic lowering of another 40 to 50 m starts in the latest Berriasian and continues into the Valanginian, the sea level reaching its lowest level of the Cretaceous Period (dropping to ~65–75 m above PDMSL) in the mid Valanginian. In the late Valanginian the level begins to rise once again with a major upward surge through the Hauterivian, culminating in the first long-term high of the Cretaceous (approaching ~160–170 m above PDMSL) in the early Barremian. In the remainder of this Stage the long-term sea level falls by ~20 m and then goes through a long period stasis for nearly 20 Myr (through Aptian and early Albian) when it only varies by relatively small amount (~15 m). This eustato-stasis changes in the late Albian when the sea level begins to rise rapidly to a high of ~205–215 m above PDMSL by the end of Albian. Levels remained relatively high in the early Cenomanian (varying only by ~20 m), undergoing a second rise in the late Cenomanian, to culminate in the highest sea levels of the Cretaceous Period (~240–250 m above PDMSL) just beyond the Cenomanian–Turonian boundary within the earliest Turonian. From this all time high the sea level fell by ~60 m by the end of Turonian, thereafter entering into another long period of stasis of nearly 20 Myr (Coniacian through Campanian), when the long-term levels vary by only ~20 m. Beginning in the Maastrichtian the sea-level shows a gradual fall of ~40 to 50 m, so that by the end of the Cretaceous it stood at ~190–200 m above PDMSL. This steady decline continues into the Danian.

The short-term sea-level curve displays considerable variation in both amplitude and duration of 3rd-order events. 58 third-order events have been identified in the Cretaceous, most of which have been documented to occur in several basins, while a smaller number have not been widely documented but are strongly indicated as being global (and included provisionally in the cycle chart). The average amplitude of sea-level falls varies from as small as 20 m to a maximum of just over 100 m and the duration varies between 0.5 Myr and 3 Myr, most of the sequences spanning 1 to 2 Myr. Average duration for 3rd-order sequences in the Cretaceous is 1.38 Myr/cycle.

Fourth-order cyclicity (~400 Kyr in duration), which most likely represents the long-period orbital eccentricity control on deposition cycles, has been documented almost throughout the Cretaceous Period. Examples of these regularly occurring 4th-order cycles have been reported from the European basins by Hardenbol et al. (1998); from the Berriasian through the early Barremian interval and again in the early Albian from the Berriasian and Valanginian sections in Switzerland and France by Strasser et al. (2000); from the Hauterivian and Albian of the Russian Platform by Sahagian et al. (1996); from late Aptian of Arabian Platform by Maurer et al. (2013); from the Albian of Oman by Immenhauser (2005); from the Cenomanian of eastern India's Cauvery Basin by Gale et al. (2002); and from the Santonian sections in the Apennines in Italy by Buonocunto et al. (1999). Fourth-order cyclicity has also been observed elsewhere in the Paleozoic (see, e.g., Haq and Schutter, 2008) and in the Cenozoic (see, e.g., Hardenbol et al., 1998) and reported most recently from the Early Jurassic by a restudy of the Mochras borehole in West Wales (Hesselbo et al., 2013). It is apparent that whenever sedimentation rates are high and fill the available depositional accommodation, 4th-order cyclicity is likely to be preserved (assumed to be modulated by long-term eccentricity and thus, climatically controlled).

Conversely, causes for third-order cyclicity (time-synchronous sea level falls of ~20 to 110 m on ~0.5 to 3 Myr time scales) in the Cretaceous world, where we lack direct evidence for major ice caps, remain cloaked in mystery. While the extended period solid-earth tectonic influences can explain the longer time-scale variations (i.e., the longer-term sea level envelope) synchronous third-order events are not easily explained. This has not stopped many authors to invoke ice accumulation on Antarctica as the primary driver of eustasy in the Cretaceous. Currently the opinion is, however, split between ice-volume supporters and skeptics. Peter Vail and his Exxon colleagues (see e.g., Vail et al., 1977) were tempted to explain third-order fluctuations in terms of glaciation, but later authors (e.g., Haq et al., 1987) left the question open. Using $\delta^{18}O$ data as evidence for ice accumulation, Matthews and Poore (1980) and Matthews (1984) had already argued for ephemeral ice sheets on Antarctica in the Late Cretaceous and Paleogene, as did Stoll and Schrag (1996) for ice in the Early Cretaceous, and again (Stoll and Schrag, 2000) for ice in the Late Cretaceous. Abreu et al. (1998) interpreted the benthic isotopic data to imply polar ice as far back as Aptian. K. Miller and his colleagues also espoused ephemeral ice-sheets during cold "snaps" (see, e.g., Miller et al., 2005a, 2008) in the predominantly greenhouse world of the Late Cretaceous. Similarly, Immenhauser (2005) held high altitude glaciation as one of several possible mechanisms that could be responsible for rapid sea-level changes in the Cretaceous. Bornemann et al. (2008) presented data showing a prominent positive oxygen-isotopic shift in the Turonian from tropical Atlantic where they inferred a glacial period lasting 200 Kyr, with ice sheets half the size of present-day Antarctic ice cap. Maurer et al. (2013) also ascribed a 5-Myr late Aptian lowstand on Arabian Plate, with 4th-order cyclic sedimentation, to glacio-eustasy and as the longest Cretaceous cooling phase. Huber et al. (2002) have disagreed with such assessments and maintained that oxygen-isotopic data from well-preserved benthic foraminiferal specimens in deep sea cores imply warm to very warm (reaching up to 20 °C in Cenomanian) Cretaceous bottom temperatures that are irreconcilable with a significant ice sheets. More recently, oxygen isotopic data from well-preserved foraminifers (that show no apparent signs of diagenesis) obtained from the Turonian in Tanzania (MacLeod et al., 2013) is at variance with isotopic records from other sites, and supports the Huber et al.'s (2002) argument. These new data show very little variation in isotopic values suggesting a relatively stable and warm Turonian that has been interpreted to imply a lack of ice sheets on Antarctica. However, the intriguing possibility that this variance between different sites could have its origin in the $\delta^{18}O$ signal being strongly controlled by ITCZ shifts (see discussion above in "Foraminiferal oxygen isotopes as a proxy for ice volume") needs to be further investigated. Thus, at this stage the issue of the cause(s) of rapid and apparently synchronous, sea-level variations in the Cretaceous remains unresolved. Implications of dynamic topography, discussed earlier, only resolve the reason for differences in the estimates of amplitudes on different margins and interior basins, but do not negate the potential of synchroniety of events in these regions. Rather, the insight gained by geodynamic modeling is that any underlying global signal of eustatic variations is likely to be altered (either negatively or positively) by dynamic topographic effects in any given location, as illustrated by the New Jersey margin.

7. Conclusions

This reevaluation of global stratigraphic data has shown that the Cretaceous world clearly exhibits widely-distributed and geologically coeval sea-level change events leading to the conclusion that *eustasy* cannot be dismissed in this largely greenhouse period. Nevertheless,

the reason(s) for relatively rapid, and at times major, sea-level falls during the Cretaceous remain unresolved. The presence of ephemeral ice sheets on Antarctica as the main driving mechanism for these changes also cannot be totally written off, but the idea has suffered a setback by the discovery of Turonian pristine foraminiferal tests whose oxygen isotopic values show little variation, implying a lack of glacioeustasy. For the same reason (i.e., paucity of ice sheets) the Cretaceous may represent an ideal record to test various geodynamic models without the complication of Northern Hemisphere ice cover or major ice sheets on Antarctica.

Consideration of various solid-earth factors that can influence sea-level change leads to the awareness that although numerous tectonic factors affect the long-term eustatic envelope, as well as local variations on very short time scales, none of these factors can explain the apparently synchronous and relatively rapid sea-level falls on third-order time scales. However, dynamic topography is relevant, in that the longer-period and long wavelength warping of margins and interior basins produce regional vertical anomalies that can dramatically alter the local physical measure of sea-level rises and falls. This leads to the conclusion that *eustatic* amplitude cannot be gleaned from any given single basin or margin and that at such locations *all measures of sea-level change are eurybatic and not eustatic*. Thus, insights gained from dynamic topography have led to the reconciliation for variance between amplitude measures of eurybatic shifts in any given region with averaged global estimates of eustatic changes.

The documented ~400 Kyr variations in sea-level (fourth-order cyclicity) through most of the Cretaceous (and elsewhere in the Paleozoic, Jurassic and Cenozoic) strongly suggests that the 400 Kyr cyclicity, presumably driven by long-term orbital eccentricity, may be a fundamental feature of depositional sequences throughout the Phanerozoic.

Acknowledgments

This paper in dedicated to one of world's leading expert on the Cretaceous Period, a role model for many paleoceanographers, and a personal friend, William W. Hay. The author acknowledges Clint Conrad (Hawaii), William Hay (Colorado), Brian Huber (Smithsonian), Howard Spero (Davis) and James Ogg (Purdue) for reviews of this paper and for pointing out important sources of information. This paper was completed while on mini-sabbaticals during the summers of 2012 and 2013 at the University of Copenhagen, and thanks are due to Hans Thybo for arranging those visits and making me feel extremely welcome in Denmark. Figures were diligently drafted by Alex Lethiers at the University of Paris.

Appendix A

Documentation of Cretaceous eustatic events

In this section the events that are considered eustatic (of global extent) are listed. For the sake of continuity with the Cretaceous, the cycle chart (Figs. 1 and 2, see also the complete colored version for the whole Cretaceous, Fig.4, appended here) includes eustatic events from the latest Jurassic (Tithonian Stage) and the earliest Paleogene (Danian Stage).

To be considered *eustatic* (as opposed to being merely local/regional, i.e., *eurybatic* shift) the occurrence of a time-synchronous event has to be widespread (e.g., if it occurs in three or more, preferably non-contiguous, basins). However, here we include several events that do not strictly fit this criterion, but are strongly suspected to be eustatic (see reason for inclusion in individual event descriptions below). These provisional "eustatic" events (which are shown with dashed lines on the cycle chart) will await confirmation from other basins. A numbering system modified from Hardenbol et al. (1998; also recommended by Snedden and Liu, 2010) for the events depicted on the cycle chart is adapted here, however, the prefixes J (for Jurassic), K (for Cretaceous) and P (for Paleogene) are added to the first two letters of the Stage names which are numbered (from oldest to youngest sequence boundaries within each Stage). The ages of the sequence boundaries are based on biostratigraphic zonations, as cross-correlated by Hardenbol et al. (1998) and Ogg and Hinnov (2012). For events occurring in an identified biozone of a singular fossil group, a mean age for the zonal duration is used (thus, in principle the ages of the events can be placed anywhere within the zonal duration). At other times it was possible to obtain more refined age estimates by using overlapping multiple fossil zonal criteria. Often it was also possible to narrow down the ages by using oxygen-isotopic trends (see text for discussion). Fig. 3, at the end of the Appendix A, shows the oxygen-isotopic data from the Contessa section (supplied by Dan Schrag, personal communication, 2006), smoothed to show prominent $\delta^{18}O$ excursions that aided in determining the timing of sequence boundaries within long-duration biozones.

Two earlier syntheses (Haq et al., 1988, and the update by Hardenbol et al., 1998), both recalibrated to GTS2012, form the core basis of the current synthesis. Haq et al. (1988, p. 107) listed the Cretaceous sequences studied by them in Switzerland, France, Belgium, the Netherlands, the US Western Interior (Colorado and Utah) as well as West Texas. For their Cretaceous recalibrations Hardenbol et al. (1998) considered the sections in the western European basins from North Sea to Italy. Jacquin et al. (1998) and Hardenbol and Robaszynski (1998) presented overviews Early and Late Cretaceous of the European basins, respectively.

Events considered eustatic are listed for each Stage with the list of sections and the relevant references where the principle documentation is derived from. For brevity, references are numbered and listed at the end of the Appendix A. A complete list of citations can be found at the end of the main body of the paper and not repeated in the Appendix A.

Early Cretaceous

The documentation for Early Cretaceous events is largely from the western European basins, the Russian Platform and the Arabian Platform, sometimes substantiated by data from the US and the Pacific. However, as discussed in the main body of the paper, oxygen-isotopic trends (considered to be largely a global signal) though unreliable in quantifying the amplitude of sea-level change, are often helpful in pinning-down the timing of events in the early Cretaceous. Prominent isotopic shifts are therefore added to the provisional list of presumed eustatic events, awaiting confirmation from stratigraphic studies.

Berriasian

KBe1 (143.9 Ma): This early Berriasian event was identified as a relatively minor sea-level fall in the western European basins (by Hardenbol et al., 1998, reference **1**) as well as from the Russian Platform (Sahagian et al., 1996, reference **2**). However, it is also indicated by oxygen-isotopic data and is therefore included provisionally as a eustatic event. **KBe2**(142.7 Ma): This relative medium amplitude event was identified both by Haq et al., 1988 (**3**) and Hardenbol et al. (**1**) in the European basins. It was also documented on the Arabian Platform by Haq and Al-Qahtani, 2005 (**4**) and is indicated by a positive excursion in the oxygen-isotopic data. **KBe3** (141.3 Ma): This event has been identified in the western European basins by **1** & **3** and on the Russian Platform by **2** and also indicated by oxygen-isotopic data. **KBe4** (140.2 Ma): Documented in western European basins (**1, 3**), on the Russian Platform (**2**), Arabian Platform (**4**) and Exmouth Plateau, offshore Western Australia in the Indian Ocean (Haq et al., 1992, reference **5**). Events KBe2 through KBe4 are also associated with 4th-order (400 Kyr) cyclicity in the European basins as shown by of Hardenbol et al. (**1**). On average all events from KBe2–KBe4 are considered to be of relatively medium magnitude (i.e., sea-level falls and rises between 25 and 75 m).

Valanginian

KVa1(139 Ma): This prominent earliest Valanginian event was documented from European basins (**1**, **3**) Arabian platform (**4**), Exmouth Plateau (**5**). In addition it is also indicated by oxygen-isotopic trends. **KVa2** (138 Ma): This event was documented from the Russian Platform (**2**) and indicated by oxygen-isotopic data. It is therefore only provisionally included in the list here. Fourth-order (400 Kyr) cycles are also seen associated with this event on the Russian Platform. **KVa3** (136.4 Ma) was documented from western European basins (**1**) and indicated by oxygen-isotopic trends. The late Valanginian transgression following this event was also documented worldwide by Cooper (1977, reference **6**) who showed it also occurring outside Europe in Afghanistan, Mekran coast in Pakistan, east coast of Africa, Madagascar, Argentina, Chile, Peru, Canadian and US Western Interior and Mexico. **KVa4** (134.2 Ma) third-order event has been documented in western European basins (**1**, **3**), the Russian Platform (**2**) and the Arabian Platform (**4**). Provincial event KVa2 is identified as of relatively minor amplitude (<25 m of sea-level fall), while the other three fall in the median magnitude range (25–75 m).

Hauterivian

Three Hauterivian events, **KHa1** (133.2 Ma), **KHa2** (132.8 Ma) and **KHa3** (131.8 Ma) have been identified in the western European basins (**1**, **3**). Two of these, KHa1 and KHa2 have also been identified on the Russian Platform (**2**), and the oldest, KHa1, is in addition indicated by oxygen-isotopic data. In the western Europe Hauterivian is also characterized by 4th-order cyclicity (**1**). KHa1 and KHa3 are of relative median amplitude, while KHa2 is considered minor.

Barremian

KBa1 (130.6 Ma): This relatively medium amplitude (25–75 m) event has been identified in the western European basins (**1**, **3**), on the Arabian Platform (**4**) and is also indicated by oxygen-isotopic trends. **KBa2** (129.9 Ma) and **KBa3** (129.4 Ma) are both of relatively minor amplitude (<25 m) and may also end up being a 4th-order events. They are included here because they have been recorded in western European basins (**1**) and on the Exmouth Plateau (**5**). KBa2 is also indicated by oxygen-isotopic data. **KBa4** (128.4 Ma) is a medium amplitude event reported from the European basins (**1**, **3**), the Exmouth Plateau (**5**) and Arabian Platform (**4** and van Buchem et al., 2010, reference **7**). **KBa5** (126.4 Ma): This late Barremian event is of relatively major amplitude (>75 m). It has been reported from the European basins (**1**, **3**) and outside Europe from the Pacific guyots (Röhl and Ogg, 1996, reference **8**), Arabian Platform (**4** and Maurer et al., 2013, reference **9**) and Exmouth Plateau (**5**). It is also indicated by oxygen-isotopic data.

Aptian

KAp1 (125.6 Ma) is a major amplitude (>75 m) event reported from the western European basins (**1**, **3**), Russian Platform (**2**) and outside Europe from eastern coasts of Africa and India, Afghanistan, Japan and British Columbia (**6**), the Pacific guyots (**8**), Exmouth Plateau (**5**) and the US Gulf Coast (Yurewicz et al., 1993, reference **10**). It is also indicated by oxygen-isotopic data. **KAp2** (123 Ma) is of relative medium amplitude (25–75 m) and has been recorded in the western European basins (**1**, **3**), the Arabian Platform (**5**, **7**), the Russian Platform (**2**) and indicated by oxygen-isotopic trends. **KAp3** (121.3 Ma) is a medium magnitude event that is included provisionally as eustatic because it was recorded from the Arabian Platform (**5**, **9**) and indicated by oxygen-isotopic data. **KAp4** (118.2 Ma) is a medium to major magnitude event that has been recorded from the western European basins (**1**), Arabian Platform (**4, 9**) and Pacific guyots (**8**). **KAp5** (116.4 Ma) and **KAp6** (115.1 Ma) are two events that are provisionally included here as medium amplitude events that are indicated by prominent positive $\delta^{18}O$ shifts and may therefore prove to be eustatic. The youngest of the Aptian events **KAp7** (113.3 Ma) is considered to a prominent major sea-level fall. It's been studied in western European basin (**1**), on the Arabian Platform (**4, 7**), the Pacific guyots (**8**), and indicated by oxygen-isotopic trends.

Albian

KAl1 (111.2 Ma): This medium amplitude event is recorded in the western European basins (**1, 3**) Arabian Platform (**4, 9**), US Gulf Coast (**3, 10**), and in Zululand, Russia and Japan (**6**). **KAl2** (110.6 Ma) and **KAl3** (109.3) events are also recorded from western Europe and Arabian Platform, but in addition are also reported from the Pacific guyots (**8**), Russian Platform (**2**) and indicated by oxygen-isotopic trends. The former has also been reported from the US Gulf Coast (**3, 10**). **KAl4** (107.5 Ma) has also been recorded from the western European basins (**1, 3**), Russian Platform (**2**) and the US Gulf Coast (**3**), as well as indicated by an oxygen-isotopic shift. **KAl5** (105 Ma) is reported from the western European basins (**1, 3**) and recorded in the US Western Interior as well as the Gulf Coast (**3, 10**). **KAl6** (103.8) has only been recorded in western European basins (**1**), but it is also a prominent oxygen-isotopic shift and thus provisionally included here. **KAl7** (103 Ma) occurs in Western European basins (**1**), Arabian Platform (**4**), Pacific guyots (**8**) and Cauvery Basin in India (Gale et al., 2002, reference **11**). It is also reinforced by an oxygen-isotopic shift of this age. Like the preceding event, **KAl8 (**100.6 Ma) is also recorded from western European basins and India, as well as being reported from the Russian Platform (**2**) and indicated by a positive $\delta^{18}O$ shift. Almost all of the Albian events can be classed as medium in magnitude (between 25 and 75 m), with the exception of KAl2 and KAl5 that are relative minor (<25 m) and the youngest KAl8, which is relatively a major (>75 m) event.

Late Cretaceous

For the Late Cretaceous the documentation of listed events increases when compared to Early Cretaceous and most Late Cretaceous stages are well studied (with the exception of perhaps Campanian). As in the Early Cretaceous, positive shifts in oxygen-isotopic values have been helpful in pinning-down the timing of events in the Late Cretaceous events.

Cenomanian

KCe1 (99 Ma) has been recorded in the western European basins (**1**, **11**) and India (**11**) and is therefore provisionally included here, awaiting confirmation from other areas. It is considered to be of relatively minor amplitude (<25 m). **KCe2** (98.4 Ma), a medium amplitude (25–75 m) event, has been reported from Western Europe (**1, 3, 11**), New Jersey margin (**12**), India (**11**). It is also recorded in oxygen-isotopic data. Like KCe1, **KCe3** (97 Ma) is also a relatively minor shift (<25), which has so far only reported western Europe and India (**11**) and indicated by oxygen-isotopic data and thus provisionally included in the current list of eustatic events. **KCe4** (95.5 Ma) is a major magnitude (>75 m) event that has been recorded in European basins (**1**, **3, 11**), on the New Jersey margin (Miller et al., 2003, 2005b, reference **12**), India (**11**), Arabian Platform (**4**) and the US Gulf Coast (**10**). It is also indicated by a prominent oxygen-isotopic shift. **KCe5** (94.4 Ma) is a relatively minor amplitude event in most places and, like KCe4, it is reported from Western Europe, New Jersey, India, Arabian Platform and in the oxygen-isotopic data. In addition, it has also been recorded in global reef/carbonate-platform data by Philip and Airaud-Crumiere (1991, reference **13**). Gale et al. (**11**) show 4th-order (400 Kyr) cyclicity to exist in the Cenomanian of the Cauvery Basin in India and they thus hypothesize a probable glacioeustatic origin for these cycles.

Turonian

KTu1 (93.8 Ma) is a relatively minor magnitude (<25 m) event that has been recorded by Gale et al., 2002 (**11**) from northern Europe and

the Cauvery Basin in India. It is also indicated by oxygen-isotopic data and therefore included here provisionally pending confirmation from other stratigraphic sections. **KTu2** (93.2 Ma) is of medium range in amplitude (25–75 m) and has been more widely recorded, i.e., from western European basins (**1, 11**), India (**11**), Arabian Platform (**4**) and global reef data (**13**). It is also reinforced by the oxygen isotopic trends. **KTu3** (92.6 Ma) is relatively minor amplitude-wise and reported from western European sections (**1, 3**), Russian Platform (**2**) and New Jersey margin (**12**). **KTu4** (91.8 Ma) is of relatively major amplitude (>75 m) recorded in western European basins (**1, 3**), Gulf Coast and New Jersey margins (**10, 12**), in the global reef/carbonate platform data (**13**), and indicated by oxygen-isotopic trends. **KTu5** (89.9 Ma) is also recorded from Western Europe, New Jersey and in isotopic data, and in addition is also reported from the Russian Platform (**2**).

Coniacian

KCo1 (88.7 Ma) has been reported from western European basins by Hardenbol et al. (**1**) as a relatively minor amplitude event. It is also recorded on the Russian Platform (**2**)as a medium amplitude fall, while the oxygen-isotopic data shows a major positive shift of this age. **KCo2** (87 Ma) is only provisionally included here since it is a prominent positive oxygen-isotopic shift. This will have to await confirmation from stratigraphic sections.

Santonian

KSa1 (86. 2 ma) is recorded from western European basins (**1, 3**), the Arabian Platform (**4**) and New Jersey margin (**12**). In addition, it can also be correlated to a positive $\delta^{18}O$ shift in the isotopic data. It is considered to be a relatively medium-range (25–75 m) eustatic fall. **KSa2** (85.3 Ma) on the other hand is a minor fall (<25 m) that has been recorded from the European basins and Russian Platform (**1, 2**). In addition it is also inferred to have occurred in New Zealand by Crampton et al. (2006, reference **14**). They used quantitative biostratigraphic technique, where clustering of events it deduced to occur near sequence boundaries. Ten of the fifteen clusters coincide with sequence boundaries in Northern Hemisphere and are inferred to be eustatic. Eight of these events in Coniacian through Maastrichtian interval coincide with eustatic events listed here. **KSa3** (84 Ma) is a medium-range (25–75 m) event that has been reported from western European basins (**1, 3**), Russian Platform (**2**), Sinai in Egypt (Lüming et al., 1998, reference **15**), Gulf of Mexico and New Jersey margins (**10, 12**) as well as New Zealand (**14**).

Campanian

Events **KCa1** (82.6 Ma) and **KCa2** (81 Ma) are both minor that have been recorded in the western European basins (**1, 3**), on the Arabian Platform (**4**) and in New Zealand (**14**). **KCa3** (80 Ma) is also reported from the European basins and Arabian Platform, but in addition it is also indicated by oxygen-isotopic data. It is of medium range (25–75 m) in amplitude. The minor (<25 m) event **KCa4a** (78.4 Ma) occurs in western European basins, the Arabian Platform and on New Jersey margin. It has also been reported from Egypt (**15**) and New Zealand (**14**) and indicated by oxygen isotopic data. In most places it is paired with a 4th-order cycle dated at 78.8 Ma. **KCa5** (76.6 Ma) has been documented only from Western Europe (**1**), however, it also correlates with a prominent positive $\delta^{18}O$ shift and is therefore included in the list provisionally. **KCa6** (75.4 Ma) and **KCa7** (73.6 Ma) are both recorded from western European basins (**1, 3**), Arabian Platform (**4**), New Jersey margin (**12**) and in addition they are also documented from the El Kef section in Tunisia (Li et al., 2000, reference **16**) and indicated by oxygen-isotopic data. KCa6 is also recorded in New Zealand (**14**) while KCa7 in Egypt (**15**). The former is of relatively lesser amplitude than latter, but both are considered to be within the medium (25–75 m) range.

Maastrichtian

The older two eustatic events of the Maastrichtian **KMa1** (72 Ma) and **KMa2** (70.6 Ma) have both been documented in western European basins (**1**), in Tunisia (**16**) and New Zealand (**14**). Both also correlate with oxygen-isotopic events and are considered to be of relatively minor amplitude (<25 m). **KMa3** (69.4 Ma) and **KMa4** (68.8 Ma) can be tracked in western European basins (**1**), on the Arabian Platform (**4**) and in the oxygen-isotopic trends. The former has also been recorded in New Jersey (**12**) and the latter in New Zealand (**14**). Both are considered to be of medium magnitude (25–75 m) in amplitude range. The youngest of the Maastrichtian event, **KMa5** (66.8 Ma), is also of medium amplitude (~75 m) and

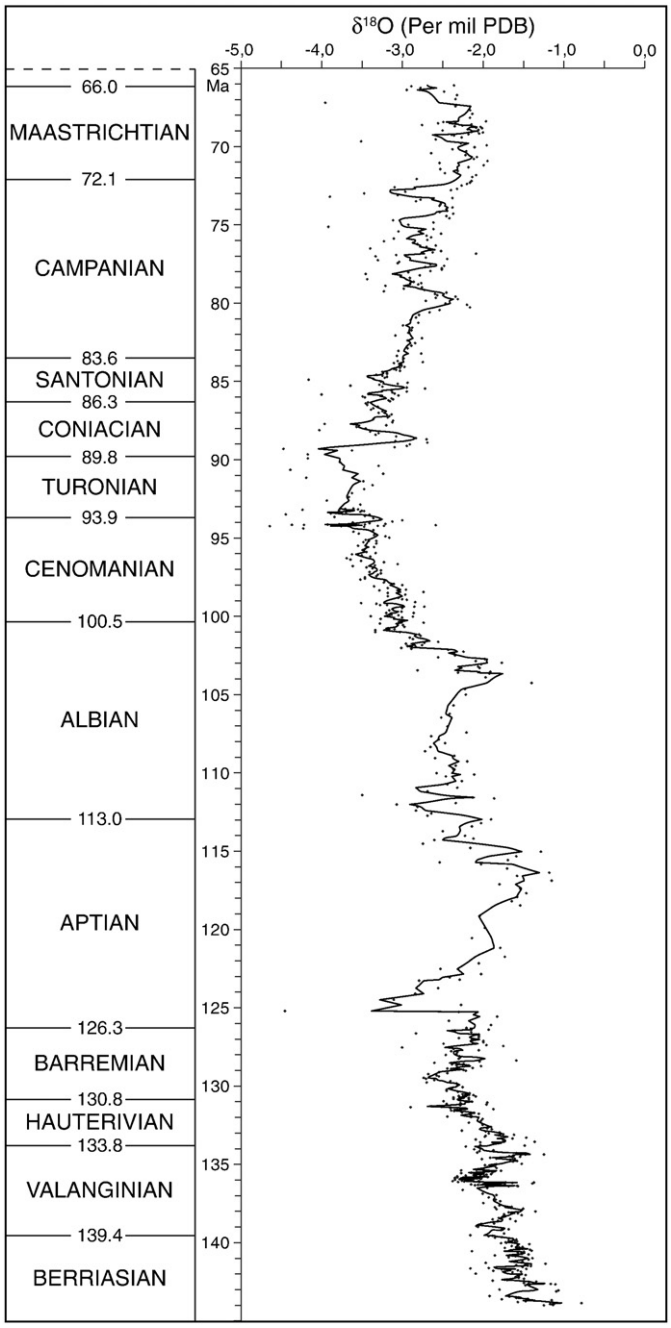

Fig. 3. Cretaceous bulk-carbonate oxygen-isotopic data from the Contessa Section, Italy (data provided by D. Schrag, personal communication, 2006). The age model for the data is constrained by foraminiferal biostratigraphy, tied to the latest Cretaceous GTS 2012 time scale (Ogg and Hinnov, 2012). The curve is a smooth (three point moving average) that reveals the broader trends in the isotopic record.

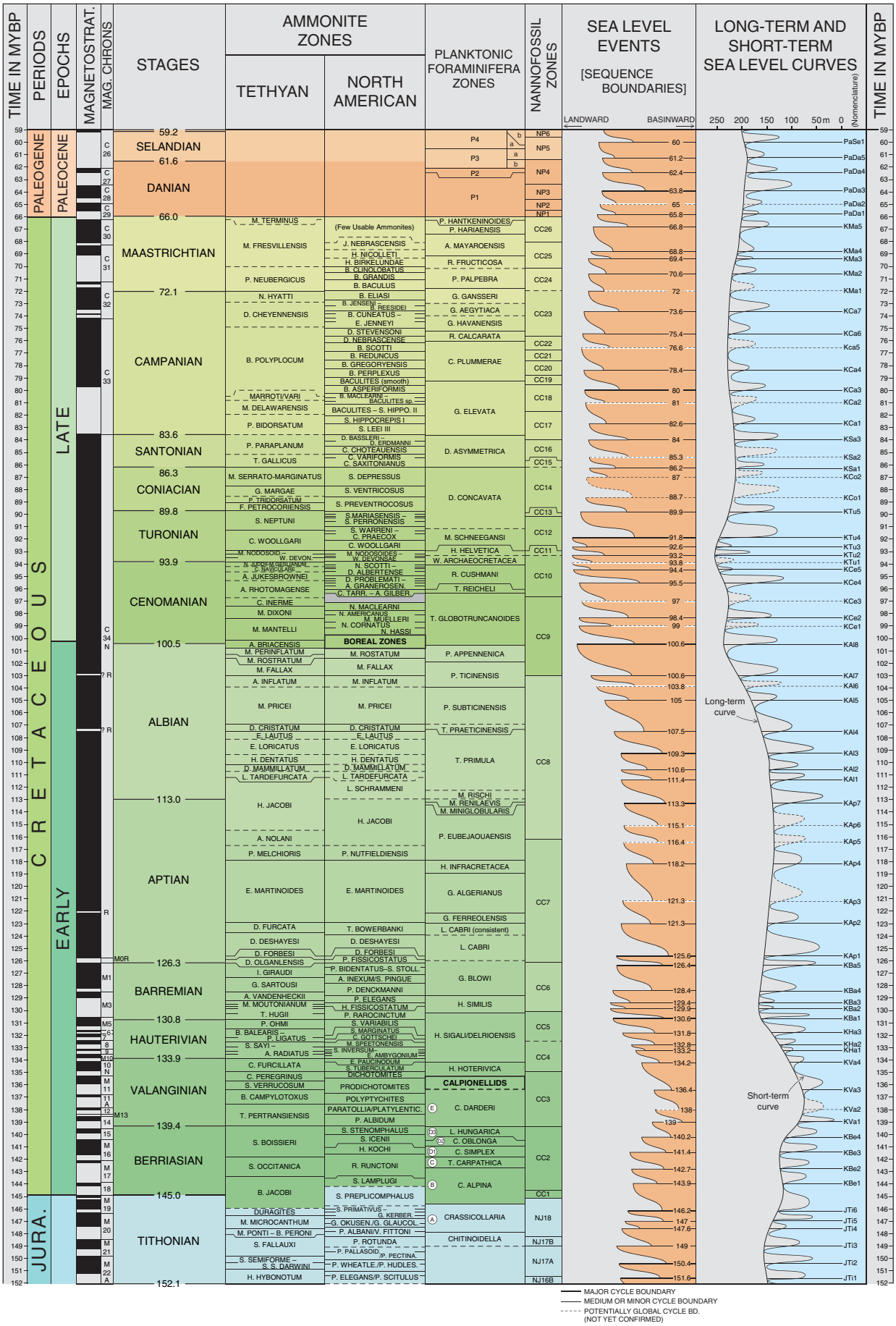

Fig. 4. A composite Cretaceous sea level curve (2013).

is seen in Western Europe (**3**), on the Arabian Platform (**4**), in Tunisia (**16**), on New Jersey margin (**12**) and in New Zealand (**14**).

References for Appendix (Numbered references in the above Appendix A, in **bold**. See main text for complete citations):

(1) Hardenbol et al. (1998) Western European basins
(2) Sahagian et al. (1996) Russian Platform and Siberia
(3) Haq et al. (1988) Western Europe, US western interior, West Texas
(4) Haq and Al-Qahtani (2005) Arabian Platform
(5) Haq et al. (1992) Exmouth Plateau, offshore western Australia, Indian Ocean
(6) Cooper (1977) Global
(7) van Buchem et al. (2010) Arabian Platform
(8) Röhl and Ogg (1996) Pacific Guyots
(9) Maurer et al. (2012) Arabian Platform
(10) Yurewicz et al. (1993) Gulf of Mexico (Mississippi and Louisiana)
(11) Gale et al. (2002) Albian–Cenomanian, NW Europe, Cauvery Basin, India
(12) Miller et al. (2003 and 2005) Late Cretaceous, New Jersey margin, US East Coast
(13) Philip and Airaud-Crumiere (1991) Global, late Cenomanian–early Turonian
(14) Crampton et al. (2006) Late Cretaceous, New Zealand
(15) Lüming et al. (1998) Late Cretaceous, Sinai, Egypt
(16) Li et al. (2000) late Cretaceous, Tunisia.

References

Abreu, V., Hardenbol, J., Haddad, G.A., Baum, G., 1998. Oxygen Isotope Synthesis: A Cretaceous Ice House? In: de Graciansky, P.-C., et al. (Eds.), Mesozoic and Cenozoic Sequence Stratigraphy of European Basins. SEPM Special Publication, 60, pp. 75–80.

Ando, A., Huber, B.T., MacLeod, K.G., et al., 2009. Blake Nose stable isotopic evidence against mid-Cenomanian glaciation hypothesis. Geology 37, 451–454.

Arbuszewski, J.A., deMenocal, P.E., Cleroux, C., Bradmiller, L., Mix, A., 2013. Meridional shifts of the Atlantic intertropical convergence zone since Last Glacial Maximum. Nat. Geosci. http://dx.doi.org/10.1038/NGEO1961.

Barrera, E., Savin, S., 1999. Evolution of late Campanian–Maastrichtian marine climates and oceans. Geol. Soc. Am. Spec. Pap. 332, 245–282.

Bornemann, A., Norris, R.G., Friedrich, O., et al., 2008. Isotopic evidence for glaciation during the Cretaceous Supergreenhouse. Science 319, 189–192.

Buonocunto, F.P., D'Argenio, B., Ferreri, V., Sandulli, R., 1999. Orbital cyclostratigraphy and sequence stratigraphy of Upper Cretaceous carbonates at Monte Sant' Erasmo, southern Apennines Italy. Cretac. Res. 20, 81–95.

Cloetingh, S., McQueen, H., Lambeck, K., 1985. On a mechanism for regional sealevel variations. Earth Planet. Sci. Lett. 75, 157–166.

Cloetingh, S., Burov, E., Francois, T., 2013. Thermo-mechanical controls on intra-plate deformation and the role of plume-folding interactions in continental topography. Gondwana Res. 24, 815–837.

Cogné, J.-P., Humler, E., Courtillot, V., 2006. Mean age of the lithosphere drives sea-level change since Pangea breakup. Earth Planet. Sci. Lett. 24, 115–122.

Conrad, C.P., 2013. The solid Earth's influence on sea level. Geol. Soc. Am. Bull. 125, 1027–1052. http://dx.doi.org/10.1130/B30764.1.

Conrad, C.P., Hager, B.H., 1997. Spatial variations in the rate of sea level rise caused by the present day melting of glaciers and ice sheets. Geophys. Res. Lett. 24, 1503–1506.

Cooper, M.R., 1977. Eustacy during the Cretaceous: its implications and importance. Palaeogeogr. Palaeoclimatol. Palaeoecol. 22, 1–60.

Crampton, J.S., Schioler, P., Roncaglia, L., 2006. Detection of Late Cretaceous eustatic signature using quantitative biostratigraphy. Geol. Soc. Am. Bull. 118, 975–990.

Emiliani, C., 1955. Pleistocene temperatures. J. Geol. 63, 538–578.

Farrell, W.E., Clark, J.A., 1976. On post-glacial sea level. Geophys. J. R. Astron. Soc. 46, 647–667.

Flament, N., Gurnis, M., Dietmar Müller, R., 2012. A review of observations and models of dynamic topography. Lithosphere 5, 189–210. http://dx.doi.org/10.1130/L245.1.

Friedrich, O., Norris, R.D., Erbacher, J., 2012. Evolution of middle to Late Cretaceous oceans—a 55 m y record of Earth's temperature and carbon cycle. Geology 40, 107–110.

Gale, A.S., 2000. The Cretaceous World. In: Culver, S.J., Rawson, P.F. (Eds.), Biotic Response to Global Change. The Last 145 Million Years. Cambridge University Press, Cambridge, pp. 4–19.

Gale, A.S., Hardenbol, J., Hathaway, B., et al., 2002. Global correlation of Cenomanian (Upper Cretaceous) sequences: evidence for Milankovitch control on sea level. Geology 30, 291–294.

Galeotti, S., Rusciadelli, G., Sprovieri, M., et al., 2009. Sea-level control on facies architecture in the Cenomanian–Coniacian Apulian margin (Western Tethys): a record of glacio-eustatic fluctuations during the Cretaceous greenhouse? Palaeogeogr. Palaeoclimatol. Palaeoecol. 278, 196–205.

Gradstein, F., Ogg, J., Smith, A. (Eds.), 2004. Geological Time Scale. Cambridge University Press (589 pp.).

Gradstein, F.M., Ogg, J.G., 2012. In: Schmitz, M.D., Ogg, G.M. (Eds.), The Geological Time Scale 2012. Elsevier, Amsterdam, p. 1176.

Gurnis, M., 1990. Ridge spreading, subduction, and sea level fluctuations. Science 250, 970–972.

Gurnis, M., 1992. Rapid continental subsidence following the initiation and evolution of subduction. Science 255, 1556–1558.

Gurnis, M., 1993. Phanerozoic marine inundation of continents driven by dynamic topography above subducting slabs. Nature 364, 754–756.

Handford, C.R., Loucks, R.G., 1993. Carbonate depositional sequences and system tracts—response of carbonate platforms to relative sea-level changes. In: Loucks, R.G., Sarg, J.F. (Eds.), Carbonate Sequence Stratigraphy. American Association of Petroleum Geologists, Memoir, 57, pp. 3–41.

Haq, B.U., Al-Qahtani, A.M., 2005. Phanerozoic cycles of sea-level change on the Arabian Platform. GeoArabia 10, 127–160.

Haq, B.U., Schutter, S.R., 2008. A chronology of Paleozoic sea-level changes. Science 322, 64–68. http://dx.doi.org/10.1126/science.116164.

Haq, B.U., Hardenbol, J., Vail, P.R., 1987. Chronology of fluctuating sea levels since the Triassic. Science 235, 1156–1167.

Haq, B.U., Hardenbol, J., Vail, P.R., 1988. Mesozoic and Cenozoic chronostratigraphy and cycles of sea-level change. Soc. Econ. Paleontol. Mineral. 42, 71–108.

Haq, B.U., Boyd, R., Exon, N.F., von Rad, U., 1992. Evolution of the Central Exmouth Plateau—a post-drilling perspective. Proc. Ocean Drill. Proj. Sci. Results 122, 801–816.

Hardenbol, J., Robaszynski, F., 1998. Introduction to the Upper Cretaceous. In: de Graciansky, P.-C., et al. (Eds.), Mesozoic and Cenozoic Sequence Stratigraphy of European Basins. SEPM Special Publication, 60, pp. 329–332.

Hardenbol, J., Thierry, J., Farley, M.B., et al., 1998. Mesozoic and Cenozoic sequence chronostratigraphic framework of European Basins. In: de Graciansky, P.-C., et al. (Eds.), Mesozoic and Cenozoic Sequence Stratigraphy of European Basins. SEPM Special Publication, 60, pp. 3–13 (Chart 5, "Cretaceous Chronostratigraphy").

Hay, W.W., 2008. Evolving ideas about the Cretaceous climate and ocean circulation. Cretac. Res. 29, 725–753.

Hesselbo, S.P., Bjerrum, C.J., Hinnov, L.A., et al., 2013. Mochras borehole revisited: a new global standard for Early Jurassic earth history. Scientific Drilling 16 (2013), 81–91.

Huber, B., Hodell, D.A., Hamilton, C.P., 1995. Middle-late Cretaceous climate of the southern high latitudes: stable isotopic evidence for minimal equator-to-pole thermal gradients. Geol. Soc. Am. Bull. 107, 1164–1191.

Huber, B., Norris, R.D., MacLeod, K.G., 2002. Deep-sea paleotemperature record of extreme warmth during the Cretaceous. Geology 30, 123–126.

Immenhauser, A., 2005. High-rate sea-level change during the Mesozoic: new approaches to an old problem. Sediment. Geol. 175, 277–296.

Ito, G., Clift, P.D., 1998. Subsidence and growth of Pacific Cretaceous plateaus. Earth Planet. Sci. Lett. 161, 85–100.

Jacquin, T., Rusciadelli, G., Amédro, F., et al., 1998. The North Atlantic cycle: an overview of 2nd-order transgressive/regressive facies cycles in the Lower Cretaceous of Western Europe. In: de Graciansky, P.-C., et al. (Eds.), Mesozoic and Cenozoic Sequence Stratigraphy of European Basins. SEPM Special Publication, 60, pp. 397–409.

Kominz, M.A., Miller, K.G., Browning, J.V., 1998. Long-term and short-term global Cenozoic sea-level estimates. Geology 26, 311–314.

Kominz, M.A., Browning, J.V., Miller, K.G., et al., 2008. Late Cretaceous to Miocene sea-level estimates from New Jersey and Delaware coastal plain coreholes. Basin Res. 20, 1–16. http://dx.doi.org/10:1111/j.1365-2117.2008.00354.x.

Lea, D., Martin, P.M., Pak, D.K., Spero, H.I., 2002. Reconstructing a 350 ky history of sea level using planktonic Mg/Ca and oxygen isotope records from a Cocos Ridge core. Quat. Sci. Rev. 21, 283–293.

Li, L., Keller, G., 1998. Maastrichtian climate, productivity and faunal turnovers in planktic foraminifera in South Atlantic DSDP sites 525A and 21. Mar. Micropaleontol. 33, 55–86.

Li, L., Keller, G., Stinnesbeck, W., 1999. The Late Campanian and Maastrichtian in northwestern Tunisia: paleoenvironmental inferences from lithology, macrofauna and benthic foraminifera. Cretac. Res. 20, 231–252.

Li, L., Keller, G., Adatte, G., Stinnesbeck, W., 2000. Late Cretaceous sea level changes in Tunisia: a multi-disciplinary approach. Geol. Soc. Lond. 157, 447–458.

Lithgow-Bertelloni, C., Gurnis, M., 1997. Cenozoic subsidence and uplift of continents from time-varying dynamic topography. Geology 25, 735–738.

Liu, L., Spasojevic, S., Gurnis, M., 2008. Reconstructing Farallon Plate subduction beneath North America back to Late Cretaceous. Science 322, 934–938.

Lüming, S., Marzouk, A.M., Morsi, A.M., Kuss, J., 1998. Sequence stratigraphy of the Upper Cretaceous of south-east Sinai, Egypt. Cretac. Res. 19, 153–196.

MacLeod, K.G., Huber, B.T., Berrocoso, A.J., Wender, I., 2013. A stable and hot Turonian without glacial $\delta^{18}O$ excursions in indicated by exquisitely preserved Tanzanian foraminifera. Geology 41. http://dx.doi.org/10.1130/G34510.1.

Matthews, R.K., 1984. Oxygen-isotopic record of ice-volume history: 100 million years of glacioeustatic fluctuations. AAPG Mem. 36, 97–107.

Matthews, R.K., Poore, R.Z., 1980. Tertiary $\delta^{18}O$ record and glacio-eustatic sea-level fluctuations. Geology 8, 501–504.

Maurer, F., van Buchem, F.S.P., Eberli, G., et al., 2013. Late Aptian long-lived glacio-eustatic lowstand recorded on the Arabian Plate. Terra Nova 25, 87–94 http://dx.doi.org/10.1111/ter.12009.

Miller, K.G., Mountain, G.S., Browning, J.V., et al., 1998. Cenozoic global sea-level, sequences, and the New Jersey Transect: results from coastal plain and slope drilling. Rev. Geophys. 36, 569–601.

Miller, K.G., Sugarman, P.J., Browning, J.V., et al., 2003. Late Cretaceous chronology of large, rapid sea-level changes: glacioeustasy during the greenhouse world. Geology 31, 585–588.
Miller, K.G., Sugarman, P.J., Browning, J.V., et al., 2004. Upper Cretaceous sequences and sea-level history, New Jersey coastal plain. Geol. Soc. Am. Bull. 116, 368–393.
Miller, K.G., Wright, J.D., Browning, J.V., 2005a. Visions of ice sheets in a greenhouse world. Mar. Geol. 217, 215–231.
Miller, K.G., Kominz, M.A., Browning, J.V., et al., 2005b. The Phanerozoic record of global sea-level change. Science 312, 1293–1298.
Miller, K.G., Wright, J.D., Katz, M.E., et al., 2008. A view of Antarctic ice-sheet evolution from sea-level and deep-sea isotope changes during the Late Cretaceous–Cenozoic. In: Cooper, A.K., et al. (Eds.), Antarctica: A keystone in a changing world: Proceedings of the 10th International Symposium on Antarctic Earth Sciences. The National Academies Press, Washington, DC, pp. 55–70.
Mitrovica, J.X., Beaumont, C., Jarvis, G.T., 1989. Tilting of continental interiors by dynamical effects of subduction. Tectonics 8, 1079–1094.
Mitrovica, J.X., Tamisiea, M.A., Davis, J.L., Milne, G.A., 2001. Recent mass balance of polar ice sheets inferred from patterns of global sea-level change. Nature 409, 1026–1029.
Moucha, R., Forte, A.M., Mitrovica, J.X., et al., 2008. Dynamic topography and long-term sea-level variations: there is no such thing as a stable continental platform. Earth Planet. Sci. Lett. 271, 101–108.
Müller, R.D., Sdrolias, M., Gaina, C., et al., 2008. Long-term sea-level fluctuations driven by ocean basin dynamics. Science 319, 1357–1362.
Ogg, J.G., Hinnov, L.A., 2012. Chapter 27, Cretaceous. In: Gradstein, F.M., Ogg, J.G., Schmitz, M.D., Ogg, G.M. (Eds.), The Geological Time Scale. Elsevier, Amsterdam, pp. 793–853.
Pearson, P.N., 2012. Oxygen isotopes in foraminifera: overview and historical review. In: Ivanov, L.C., Huber, B.T. (Eds.), Reconstructing Earth's Deep-time Climate. The Paleontological Society Papers, 18, pp. 1–38.
Philip, J.M., Airaud-Crumiere, C., 1991. The demise of the rudist-bearing carbonate platforms at the Cenomanian–Turonian boundary: a global control. Coral Reefs 10, 115–125.
Ridgewell, A., 2005. A Mid Mesozoic revolution the regulation of ocean chemistry. Mar. Geol. 217, 339–357.
Ritsema, J., van Heijst, J., Woodhouse, J.H., 2004. Global transition zone tomography. J. Geophys. Res. 109. http://dx.doi.org/10.1029/2003JB002610.
Röhl, U., Ogg, J.G., 1996. Aptian–Albian sea level history from guyots of western Pacific. Paleoceanography 11, 595–624.
Rowley, D.B., Forte, A.M., Moucha, R., et al., 2013. Dynamic topography change of the eastern United States since 3 million years ago. Science 340, 1560–1563.
Sahagian, D., Pinous, O., Olferiev, A., Zakharov, V., 1996. Eustatic curve for the Middle Jurassic–Cretaceous based on Russian platform and Siberian stratigraphy: zonal resolution. AAPG Bull. 80, 1433–1458.
Sarg, J.F., 1988. Carbonate sequence stratigraphy. In: Wilgus, C.K., et al. (Eds.), Sea Level Changes—An Integrated Approach. SEPM Special Publications, 42, pp. 155–181.
Schmidt, M.W., Spero, H.J., 2011. Meridional shifts in the marine ITCZ and the tropical hydrologic cycle over the last three glacial cycles. Paleoceanography 26, PA105. http://dx.doi.org/10.1029/2010PA001976.
Shackleton, N.J., 1967. Oxygen isotope analyses and Pleistocene temperatures reassessed. Nature 215, 15–17.
Sigloch, K., McQuarrie, N., Nolet, G., 2008. Two-stage subduction history under North America inferred from multiple-frequency tomography. Nat. Geosci. 1, 458–462.
Snedden, J.W., Liu, C.A., 2010. A compilation of Phanerozoic sea-level change, coastal onlaps and recommended sequence designations. Search and Discovery Article 40594. ExxonMobil Production Co.
Snedden, J.W., Liu, C., 2011. Recommendations for uniform chronostratigraphic designation system for Phanerozoic depositional sequences. Am. Assoc. Pet. Geol. Bull. 95, 1095–1122.
Southam, J., Hay, W.W., 1981. Global sedimentary mass balance and sea-level changes. In: Emiliani, C. (Ed.), The Oceanic Lithosphere. The Sea, volume 7. Wiley Interscience, New York, pp. 125–145.
Spasojevic, S., Gurnis, M., 2012. Sea level and vertical motion of continents from dynamic earth models since Late Cretaceous. AAPG Bull. 96, 2037–2064.
Spasojevic, S., Liu, L., Gurnis, M., Müller, R.D., 2008. The case for dynamic subsidence of the United States East Coast since the Eocene. Geophys. Res. Lett. 35, L08305. http://dx.doi.org/10.1029/2008GL033511.
Stoll, H.M., Schrag, D.P., 1996. Evidence of glacial control of rapid sea level changes in the Early Cretaceous. Science 272, 1771–1774.
Stoll, H.M., Schrag, D.P., 2000. High-resolution stable isotope record from Upper Cretaceous rocks of Italy and Spain: glacial episodes in a greenhouse planet? Geol. Soc. Am. Bull. 112, 308–319.
Strasser, A., Hillgärtner, H., Hug, W., Pillet, B., 2000. Third-order depositional sequence reflecting Milankovitch cyclicity. Terra Nova 12, 303–311.
Tyrrell, T., Zeebe, R.E., 2004. History of carbonate ion concentration over the last 100 million years. Geochem. Cosmochem. Acta 68, 3521–3530.
Vail, P.R., Mitchum Jr., R.M., Todd, R.G., et al., 1977. Seismic stratigraphy and global changes of sea level. AAPG Mem. 26, 49–212.
van Buchem, F.S.A.P., Al-Husseini, M.I., Maurer, F., et al., 2010. Sequence-stratigraphic synthesis of the Barremian–Aptian of the Eastern Arabian Plate and implications for the petroleum habitat. GeoArabia Spec. Publ. 4, 9–48.
Van Sickel, W.A., Kominz, M.A., Miller, K.G., Browning, J.V., 2004. Late Cretaceous and Cenozoic sea-level estimates—backstripping analysis of borehole data. Basin Res. 16, 451–465.
Van Wagoner, J.C., Posamentier, H.W., Mitchum, R.M., 1988. An overview of the fundamentals of sequence stratigraphy. In: Wilgus, C.K., et al. (Eds.), Sea Level Changes—An Integrated Approach. SEPM Special Publications, 42, pp. 39–45.
Yurewicz, D.A., Marler, T.B., Meyerholtz, K.A., Siroky, F.X., 1993. Early Cretaceous carbonate platform, north rim of the Gulf of Mexico, Mississippi and Louisiana. In: Simo, J.A.T., Scott, R.W., Masse, J.-P. (Eds.), Cretaceous Carbonate Platforms. AAPG Memoir, 56, pp. 81–96.
Zeebe, R.E., 2001. Seawater pH and isotopic paleotemperatures of Cretaceous oceans. Palaeogeogr. Palaeoclimatol. Palaeoecol. 170, 49–57.